

# **Stony Brook University**



OFFICIAL COPY

**The official electronic file of this thesis or dissertation is maintained by the University Libraries on behalf of The Graduate School at Stony Brook University.**

**© All Rights Reserved by Author.**

**Radium Isotopes as Tracers of Pore Water Dynamics in Two Long Island Salt Marsh  
Systems**

A Thesis Presented

by

Camilo Salazar

to

The Graduate School

in Partial Fulfillment of the Requirements

for the Degree of

Master of Science

in

Marine and Atmospheric Science

Stony Brook University

August 2015

**Stony Brook University**

The Graduate School

Camilo Salazar

We, the thesis committee for the above candidate for the  
Master of Science degree, hereby recommend  
acceptance of this thesis.

J. Kirk Cochran, Professor  
School of Marine and Atmospheric Science  
Stony Brook University

Henry J. Bokuniewicz, Professor  
School of Marine and Atmospheric Science  
Stony Brook University

Robert Aller, Distinguished Professor  
School of Marine and Atmospheric Science  
Stony Brook University

This thesis is accepted by the Graduate School

Charles Taber  
Dean of the Graduate School

Abstract of the Thesis

**Radium Isotopes as Tracers of Pore water Dynamics in Two Long Island Salt Marsh**

**Systems**

by

Camilo Salazar

Master of Science

in

Marine and Atmospheric Science

Stony Brook University

2015

A study of pore water residence time as traced by short-lived radium (Ra) isotopes ( $^{224}\text{Ra}$  and  $^{223}\text{Ra}$ ) was conducted on two marsh systems in the south shore of Long Island, New York. Pore water was collected in July (summer) and November-December (winter) of 2013 at depths of 20 cm and 120 cm over three-station transects from the inner marsh to the marsh edge adjacent to a tidal channel. One of the marsh systems is the Wertheim Nationals Wildlife Refuge (NWR), from which two marshes were sampled; Wertheim 1 (W1), a restored marsh, and Wertheim 2 (W2), non-restored. The second marsh system is located at Seatuck NWR, which has been identified as in need of restoration. This study is based on the principle that short-live Ra isotopes accumulate in pore water by recoil following production from radioactive decay of parents nuclides. Thus this study assumes that the activity of Ra isotopes must reflect the length of time the pore water remains in contact with the solids as well as the geochemical conditions. Based on a transport-reaction model, the results for W1 showed average residence were 2.4 days for summer at 20 cm and 3.6 days at 120 cm, while winter showed averages of 3 days at 20 cm and 5 days at 120 cm. Shallow samples (20 cm) at the W1 marsh edge had shorter residence times than deep samples. W2 showed pore water residence times for summer of 2.6 days at 20 cm and 1.4 days at 120 cm, while winter showed 2 days at 20 cm and 1 day at 120 cm, however the spatial and temporal distribution was more evident than at W1, with shorter residence times at shallow depth at the marsh edge and mid-marsh in winter while the opposite was detected for summer, suggesting that drainage during summer is more characterized by deep flow (120 cm). Winter samples for the Wertheim marshes show shorter pore water residence times at shallow depth and the marsh edge, suggesting a possible tidal drainage effect given by proximity to the tidal channel and characterized by faster flow of pore water from the marsh edge at 20 cm than at 120 cm. The Seatuck marsh showed average pore water residence times for summer of 6 days at 20 cm and 2.6 days at 120 cm, while winter showed 6 days at 20 cm and 5 days at 120 cm. Seatuck had with longer residence times at shallow samples, and a possible spatial and temporal

pattern of decreasing residence times from the marsh edge toward the marsh interior, and longer residence times during winter. The overall pore water salinity (PSU) for Wertheim 1 was 14.2 and 15.2 for summer and winter samples respectively, however salinities were higher at 120 cm, and the salinity at the tidal channel was 8.1 for summer and 8.7 for winter. Wertheim 2 had an overall pore water salinity of 13 and 24.7 for the summer and winter samples respectively, and higher salinities were found at 20 cm depth relative to 120 cm, and the salinity at the tidal channel was 8.4 for summer and 15.2 for winter. The overall pore water salinities for Seatuck were 18.3 for summer and 20.9 for winter, and higher values were found at 20 cm depth in summer while winter showed the opposite, and the salinity at the tidal channel was 20.5 ‰ for summer and 21.4 ‰ for winter. Salinity for all the sampled marshes showed a possible spatial pattern with higher salinity pore water at deep samples at Wertheim 1 through the transect, while the opposite was found at Wertheim 2 and Seatuck. The observations on salinity suggest a possible lateral flow through the marshes. This study proposes a method to age marsh pore water at different depths that could have potential to study and compare marsh systems that require restoration or to examine the responses to modifications made through restoration activities. Most of marsh post-restoration studies and monitoring activities study look at the marsh surface area, however the geochemical processes at the rhizosphere of low-to-intertidal marsh, as well as the role of the subterranean estuary in marshes are not fully understood. Therefore there is a significant need for geochemical methods that can be integrated into pre- and post-restoration projects and improve our understanding of marsh drainage and overall hydrology.



Marsh system at the Wertheim National Wildlife Refuge, Shirley, New York. North-South view from Carmans River toward the bay. Photo by Tom Iwanejko, Suffolk County Department of Public Works, NY.

## Table of Contents

	Page
1. Introduction	1
1.1 Project Justification	3
1.2. Site description	4
1.3. Previous work	6
2. Methods	7
2.1. Pore water sampling	7
2.2. Sediment Sampling	7
2.3. Pore water sampling events	8
2.4. Water quality parameters (temperature, salinity, and dissolved oxygen)	9
2.5. Measurement of the short-lived radium isotopes ( $^{223}\text{Ra}$ and $^{224}\text{Ra}$ )	9
3. Results	9
3.1. Temperature	9
3.1.1. Summer	9
3.1.2. Winter	10
3.2. Radium	12
3.2.1. Summer	12
3.2.2. Winter	12
3.3. Salinity	14
3.3.1. Summer	14
3.3.2. Winter	14
3.3.3. Radium Isotopes versus Salinity	16
3.4. Dissolved Oxygen	17
3.4.1. Summer	17
3.4.2. Winter	17
3.4.3. Radium Isotopes versus Dissolved Oxygen	19
3.5. Solid phase radionuclide data	19

4. Discussion	21
4.1. Estimating residence times of marsh pore water using $^{224,223}\text{Ra}$	21
4.1.1. Supply of $^{224,223}\text{Ra}$ to marsh pore water	23
4.1.2. Pore water Residence Times based on $^{224}\text{Ra}$	27
4.1.3. Pore water Residence Times based on $^{223}\text{Ra}$	27
4.1.4. Possible effects of salinity on pore water Ra activities	29
4.2. Intra- and inter-marsh variations in pore water residence times	31
5. Conclusions	37
References	45



## List of Figures/Tables/Illustrations

Figure 1. A: Simple model of possible flow paths of water in a salt marsh.	3
Figure 2. Area of Study and sampling stations.	5
Figure 3. Pore water sampling methodology using a PushPoint sampler connected to a 0.5 microns filter and a 150 ml syringe.	8
Figure 4. Temperature ( $^{\circ}\text{C}$ ) for summer and winter.	11
Figure 5. Activities for $^{224}\text{Ra}$ and $^{223}\text{Ra}$ for summer and winter.	13
Figure 6. Tidal ditches and Pore water salinity values ( $\text{‰}$ ) for summer and winter.	15
Figure 7. $^{224}\text{Ra}$ and $^{223}\text{Ra}$ activities (dpm/100 L) versus salinity ( $\text{‰}$ ) for summer and winter samples.	16
Figure 8. Dissolved oxygen (DO) for summer and winter.	18
Figure 9. Radium isotopes ( $^{224}\text{Ra}$ and $^{223}\text{Ra}$ ) versus dissolved oxygen for summer and winter samples.	19
Figure 10. $^{228}\text{Th}$ and $^{235}\text{U}$ activities (dpm/g) for all marshes versus sampling stations.	20
Figure 11. Activities for $^{226,228}\text{Ra}$ from sediment samples for all marshes.	21
Figure 12. Ingrowth to steady-state activities for $^{224}\text{Ra}$ (A) and $^{223}\text{Ra}$ (B) for the three marshes: Wertheim 1, Wertheim 2, and Seatuck.	26
Figure 13. Pore water residence times determined based on $^{224}\text{Ra}$ (A, C, E) and $^{223}\text{Ra}$ (B, D, F) for summer and winter samplings.	28
Figure 14. Linear relationship between pore water residence times determined by $^{224}\text{Ra}$ versus $^{223}\text{Ra}$ . All marshes included.	29
Figure 15. Salinity versus $^{224}\text{Ra}$ -derived pore water residence times for summer and winter for Wertheim 1 (A), Wertheim 2 (B), and Seatuck (C).	30

Figure 16. Pore water flow observed for Wertheim 1 based on the simple model for pore water flow. Thicker arrows indicate faster flow or shorter pore water residence times. The interface area of fresh and salt water mixing is assumed as this study sampled at just two depths. A: winter, B: summer. MHW: mean high water, MSL: mean sea level, MLW: mean low water.	34
Figure 17. Pore water flow observed for Wertheim 2 and Seatuck based on the predicted model. Thicker arrows indicate faster flow or shorter pore water residence times. A: Wertheim 2 winter, B: Wertheim summer, Seatuck summer, and Seatuck winter. MHW: mean high water, MSL: mean sea level, MLW: mean low water.	35
Figure 18. Aerial view of the Wertheim areas in 2004 (pre-project) and 2013 (post-project). A: Wertheim 1 2004, B: Wertheim 1 2013, C: Wertheim 2 2004 (center), D: Wertheim 2 2013 (center).	36
Figure 19. Elevation contour (5 ft) and depth to Upper Glacial Aquifer (data from USGS) over a Digital Elevation Model (DEM) (data from Suffolk County) for Wertheim 1 and 2. This figure shows a possible fresh groundwater influence over Wertheim 1 (blue) from the area north-east from the site, as compared with Wertheim 2.	38
Table 1. Results for Ra isotopes (dpm/100 L) and water quality parameters in the pore water for all the marshes: salinity (‰), temperature (°C), and dissolved oxygen (mg/L).	42
Table 2: Solid phase radiochemical data and $^{224,223}\text{Ra}$ production rates.	43
Table 3. Ingrowth to steady-state activities based on calculated production rates (P) and solving for $A_{Ra}$ applying eqn. 7: $A_{Ra} = P'(1 - e^{-\lambda\tau})$	44

## **Acknowledgments**

This study was possible by the support of several organizations and their wonderful people; Mary Dempsey and Tom Iwanejko from the Office of Vector Control from the Suffolk County Department of Public Works, Monica Williams, from the National Fish and Wildlife Service, Patricia Rafferty, National Park Service.

For supporting and mentoring my journey through the School of Marine and Atmospheric Sciences, I ought to thank Dr. J. Kirk Cochran. I would also like to thank my thesis readers Dr. Henry J. Bokuniewicz and Dr. Robert Aller, professors of the School of Marine & Atmospheric Sciences, Stony Brook University.

I would like to thank Christina Heilbrun, in Dr. Cochran's Laboratory, for her dedication and support through my research.

Many thanks to the SoMAS community that made part of my academic, scientific, and social formation through my years at Stony Brook University. Special thanks to the Center for Inclusive Education for their support and motivation.

The engine and fuel for my years and achievements at Stony Brook University is of course my family. No written words can express how thankful I am for my wife Alicia and my sons; Matias and Keanu, for their love, support, motivation, and the most powerful force; the constant sense of them believing in me.

## 1. Introduction

Tidal salt marshes are considered among the most important coastal ecosystems due to their diverse environmental functions, which are closely related to their hydrodynamic and biogeochemical responses to tidal inundation, pore water (groundwater), and submarine groundwater discharge (SGD) (Koch and Gobler, 2009; Kelly et al., 2011; Donnelly and Bertness, 2001). Marsh pore water is affected by the spatial overlap of terrestrial and oceanic forces, thus fluid advection through marsh sediments may result in variable rates of marsh drainage and pore water residence times (Burnet et al. 2003). The subsurface hydrology of marshes is determined by several factors such as; topography and sediment composition and structure, groundwater flow, tidal pressure and wave action. Thus, pore water flow through marshes can be a combination of horizontal and vertical subsurface flow, however marshes are locally affected by a variety of factors that determine a predominant flow vertical or horizontal with a temporal and spatial variation. Vertical flow can be caused by tidal pressure from overlying water infiltration during high tide inundation over the marsh, increased hydrostatic pressure at depth during low tide, as a result of mixing of cold overlying water with pore water that has been warmed during low tide, bioturbation and marsh irregular topography. Horizontal pore water flow can occur as a result of groundwater flow from land sources directed by aquifer sediment structures, shallow confined permeable layers, and hydraulic head (Taillefert et al. 2007). Therefore, the hydrodynamic characterization of marsh pore water through conventional methods, such as Darcy's Law, has been complicated due to the high complexity of marsh subsurface flow. In addition, the study of marsh pore water residence time has been of increasing importance because many trace metals and dissolved nutrients such as nitrate and phosphate are cycled through marshes into coastal marine environments (Charette et al. 2005).

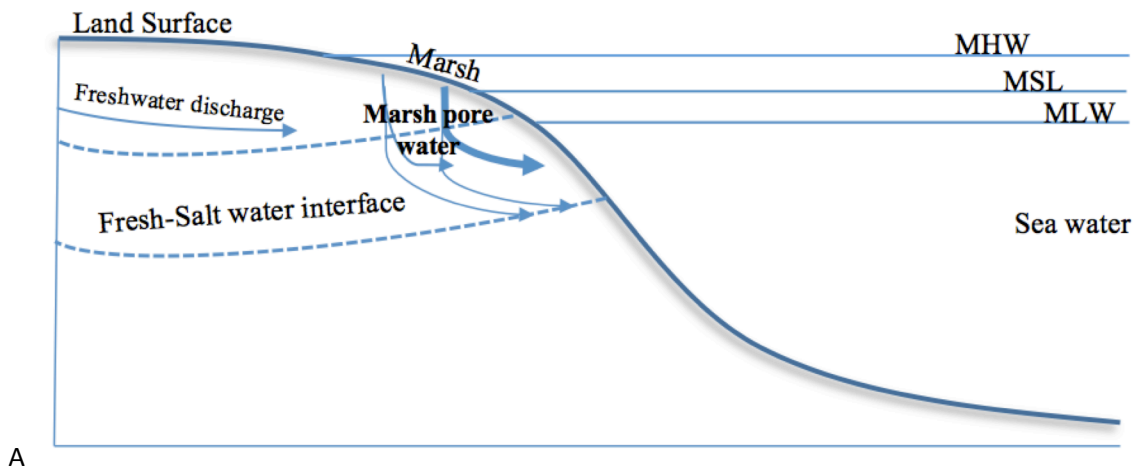
Natural geochemical tracers, such as radium (Ra) isotopes, have proven useful to describe geochemical processes in many environments, such as salt marshes (Moore, 1996; Moore, 2000a, 2000b; Charette et al., 2001; Charette, 2007, 2008). Radium isotopes are useful geochemical tracers because Ra is enriched, relative to surface water, in brackish pore water due to cation exchange processes, such that the distribution coefficient ( $K_d$ ) of Ra decreases in saline environments (Charette, 2007). Four Ra isotopes, members of the uranium and thorium decay series, have half-lives from few days to several years that make them useful tracers of many

oceanic processes ( $^{238}\text{U} \rightarrow ^{226}\text{Ra}$ :  $T_{1/2}=1600$  years;  $^{235}\text{U} \rightarrow ^{223}\text{Ra}$ :  $T_{1/2}=11.4$  days , and  $^{232}\text{Th} \rightarrow ^{228}\text{Ra}$ :  $T_{1/2}=5.75$  years  $\rightarrow ^{224}\text{Ra}$ :  $T_{1/2}=3.6$  days). These radium isotopes occur naturally and have been used as tracers to quantify SGD-derived fluxes from marshes and coastal sediments. This application is based on the fact that the Ra isotopes are recoiled from particles to pore water during their production and can also be desorbed from particle surfaces as a result of cation exchange processes during saline-fresh water mixing, thus making them suitable tracers for processes such as advection and diffusion (Krest et al. 2000; Charette et al. 2007, Garcia-Solsona et al. 2008). Therefore, Ra isotopes are potential indicators of fluxes of water as well as pore water residence time through marsh sediments.

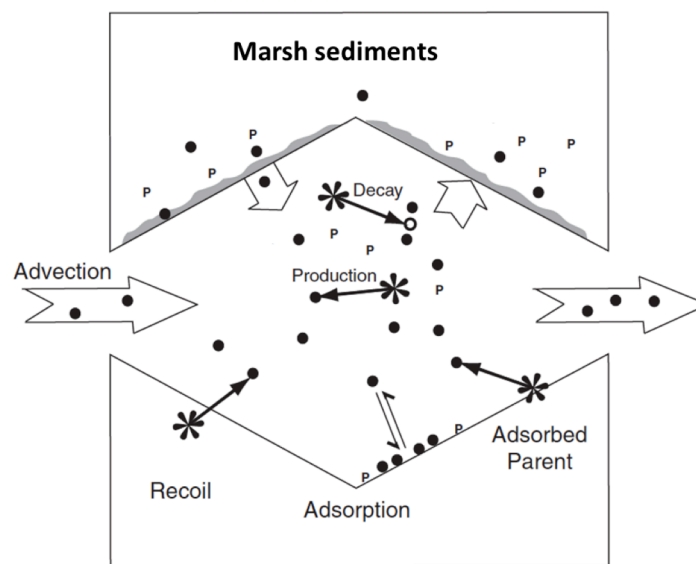
Possible flow paths of water in a salt marsh are shown in Fig. 1A. In a simple model, tidal flooding of the marsh surface drives flow vertically in the marsh and laterally toward tidal channels. This flow may be complemented by fresh water flow driven by a hydraulic gradient upland, and such flow may be preferentially occurring at depth in the marsh and have a large horizontal or lateral component.

This study uses the short-lived Ra isotopes  $^{223}\text{Ra}$  and  $^{224}\text{Ra}$ , as tools to investigate hydrological aspects of pore water in two marsh systems in Long Island. The study is based on the principle that in marsh peat, Ra produced in the marsh sediment accumulates in the pore water, eventually reaching steady state activities over times long compared with the radionuclide half-lives (Fig. 1B). We hypothesize that time scales of flow will be faster (and thus pore water residence times will be shorter) in sites close to tidal channels and near the marsh surface (Fig. 1A). The objective of this research is therefore to characterize groundwater hydrologic aspects such as pore water residence times, in the studied marshes, and to provide a better understanding on how restored marsh systems function with respect to pore water residence time.

The project areas are the Wertheim National Wildlife Refuge (Shirley, New York), which has been subjected to restoration through Integrated Marsh Management practices in 2006, and the Seatuck National Wildlife Refuge (Islip, New York), which contains a marsh system that has not been subjected to restoration activities but is suggested as a candidate for restoration. Both marsh systems are located on the south shore of Long Island, NY. Thus, this study provides a comparison between restored and non-restored marsh systems.



A



B

Figure 1. **A:** Simple model of possible flow paths of water in a salt marsh. Tidal flooding of the marsh surface drives flow vertically in the marsh and laterally toward the bay. Thicker arrows indicate faster flow and lower pore water residence time. **B:** Steady state  $^{224,223}\text{Ra}$  activities in marsh pore water are determined by recoil after production from parent nuclides;  $^{227,228}\text{Th}$ , adsorption back onto the grains as a result of cation exchange processes during saline-fresh water mixing, decay, and any loss (export) due to flow out of the marsh peat (P: parent nuclide) (modified from Porcelli, 2008).

**1.1. Project Justification:** Salt marshes form a coastal ecosystem occupied by halophytic vegetation that is exposed to characteristic hydrodynamic conditions (e.g. tidal inundation and drainage), and their environmental services are thought to be important for human and the local ecosystem (Kelly et al. 2011; Simas et al. 2001). The management and restoration of marshes is generally focused on the vegetated area and can vary from the re-introduction of tidal flow to the modification of marsh surface topography through Integrated Marsh Management (IMM) and

Open Marsh Water Management (OMWM) (Rochlin et al. 2011, 2012a, 2012b). The latter principally aims to facilitate the growth of native salt marsh vegetation and reduce the proportion of invasive or non-native plants such as common reed (*Phragmites australis*).

The assessment and monitoring of the above described restoration activities have been mostly based on ecological responses such as mosquito production, invasive plant coverage, growth of native marsh vegetation, abundance and diversity of nekton species transported by the tidal regime into marsh open water areas, and abundance and diversity of avian species (Roman et al. 2002; Rochlin et al. 2009, 2011, 2012b; Konisky et al. 2006). However there has been a lack of understanding of the biogeochemical changes in marsh sediments due to restoration practices, especially with respect to pore water residence times and drainage.

There is a general lack of information on the hydrological dynamics of pore water in marshes that have been subject to management or restoration activities. Studies on marsh restoration are mostly focused on abiotic factors such as groundwater salinity, water table, and biotic factors such as vegetation, nekton, and birds (Konisky et al. 2006). However, there is a lack of information on characterization of marsh drainage of pre- and post-restoration projects, which is of great importance as the dynamics between fresh water and salt water in the subterranean estuary determine the geochemical nature of marsh sediments, thus having an important role on the function of the marsh functions (e.g. retention, consumption, and delivery of nutrients).

In addition, the South Shore of Long Island has been indicated to be at risk of sea level rise and possible increases of storm surge and intensity. Hence this study provides valuable information to complement current efforts for preservation and restoration of tidal marshes. The approaches taken in this study are applicable not just locally but to other marsh settings as well.

**1.2. Site description:** The areas of study are two marsh systems; Wertheim NWR, composed of two marshes Wertheim 1 and Wertheim 2, and the second marsh system is one marsh located at Seatuck NWR. Wertheim 1 and 2, located within the same marsh system, are ~29 km from Seatuck, all on the South Shore of Long Island, New York, USA (Figure 2). The three marshes are managed by the United States Fish and Wildlife Service (USFWS) and they are all National Wildlife Refuges (NWR). Seatuck is located in the Town of Islip at about ~67 km east of New

York City, bordered by a populated area, Champlin Creek, and the Great South Bay. Wertheim 1 and 2 are within the Wertheim NWR in the town of Shirley at ~94 km east of New York City. These marshes show a configuration typical of New England marshes with low marsh dominated by cordgrass, *Spartina alterniflora*, and high marsh supporting cordgrass, *Spartina patens*.

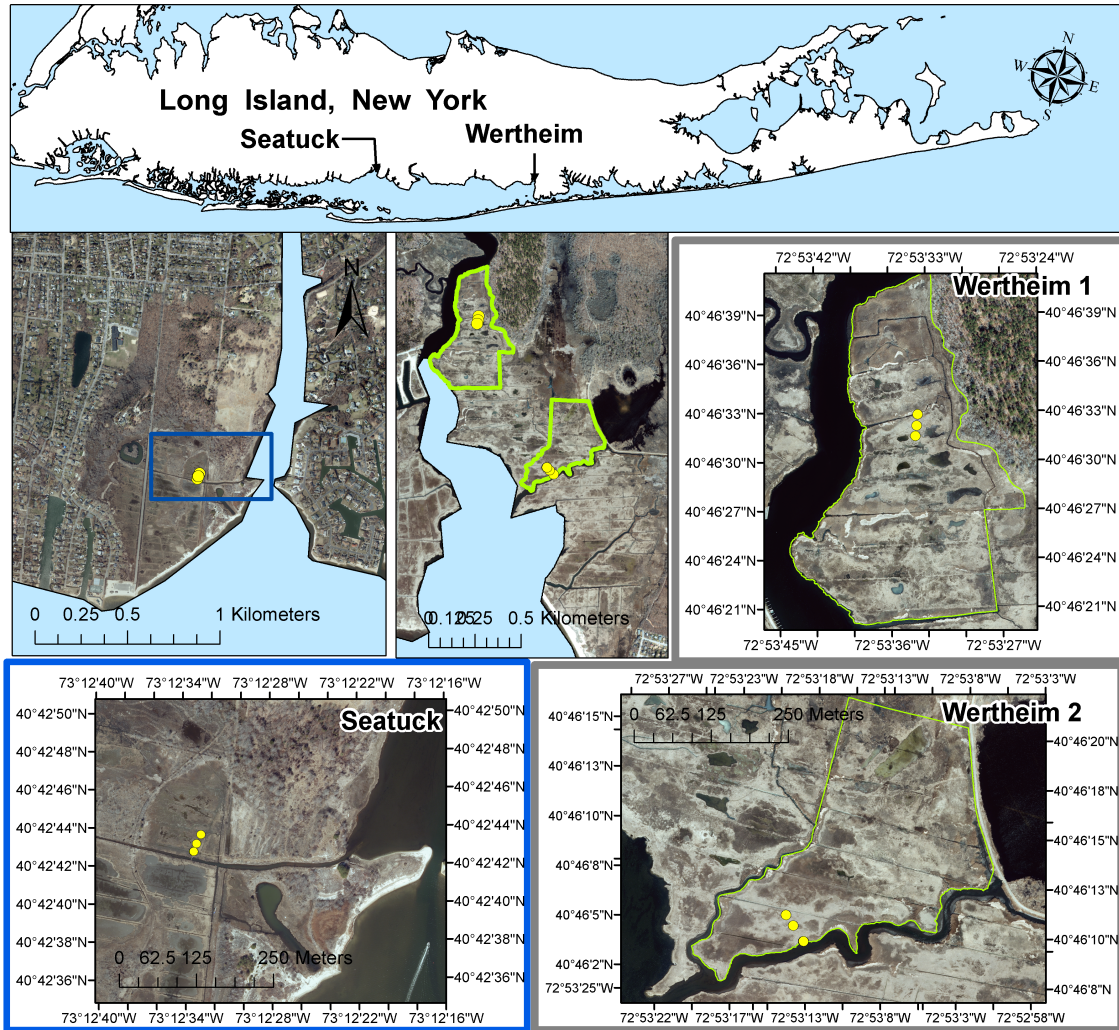


Figure 2. Area of Study and sampling stations. Samples were collected at 20 cm and 120 cm depths from each sampling location (yellow dots). Sampling stations approximately 20 meters apart. Sampling stations at the edge of the marsh at approximately 0.5 meters from the tidal channel.

The Wertheim NWR is one of the largest continuous salt marshes on Long Island, and has been subjected to a number of anthropogenic stressors including upland urbanization, grid ditching, tidal restrictions, and extensive stands of invasive *P. australis* (Rochlin et al 2012b). The tidal range for Wertheim is relatively small, with a mean range of 0.34 m and a spring range of 0.41 m



(<http://co-ops.nos.noaa.gov/tides05/tab2ec2a.html>). Wertheim is located in Shirley, NY, and it is bordered to the south by the Great South Bay with the Carmans River along the west side. The Wertheim 1 area was subjected to an integrated salt marsh management project in 2004. This consisted mainly of modification of the marsh surface area by reconfiguring the tidal flow network through creation of new hydrologic features (tidal channels and pools) and rearranging old grid ditches into naturalized (i.e., meandering ditches cut to slope), or enhanced (i.e., ditches cut to slope) tidal channels in order to enhance tidal exchange to the marsh interior and control *P. australis*. The main goals of these restoration practices were the improvement of the biological functions of the marsh and to decrease the application of pesticides applied for mosquito control.

Seatuck Wildlife Refuge is located in the town of Islip, on the South Shore of Long Island. The mean tidal range at Seatuck is 0.30 m, with the spring tidal range at 0.34 m (<http://co-ops.nos.noaa.gov/tides05/tab2ec2a.html>). Champlin Creek runs parallel to the eastern border of the marsh and the Great South Bay is the southern boundary. The vegetation is similar to a traditional New England marsh; however high marsh is a mixed of *S. alterniflora* and *S. patens*.

Because the geographical proximity of the two systems and comparable physiographic settings, many factors like historical weather events, tidal range, sediment supply, and salinities are largely similar between the three marsh systems.

**1.3. Previous work:** Radium (Ra) isotopes have been used as tracers for submarine groundwater discharge (SGD) on different coastal environments such as marshes and estuaries (Charette et al. 2003; Charette, 2007). Short-lived radium (Ra) isotopes are particularly useful to characterize some aspects of marsh hydrology, such as pore water residence time.

The south shore of Long Island has been the subject of several studies mostly focused on characterizing the flow of SGD into the Great South Bay through different methods such as vented benthic chambers, and radium budgets (Bokuniewicz and Zeitlin, 1980; Beck et al., 2007; Yang, 2008). A radium isotope budget for the Great South Bay by Beck et al. (2007), included the flux of SGD from marshes located within the areas of the Carmans and Connetquot Rivers, the main sources of fresh water to the bay. The results indicated that the marshes were not a significant source of Ra to the bay (Beck et al, 2007). However, drainage and percolation of

water through salt marshes is likely locally important as a significant factor in marsh health and resiliency.

**2. Methods:** Pore water samples were collected through a modification of the methods described by Charette (2007). Pore water samples (4 L each) were collected from 20 cm and 120 cm at each sampling location, approximately 20 m apart, and across transects on each marsh. Pore water samples were collected from two depths; 20 cm and 120 cm, at each sampling location on each marsh. The depths were determined with the intention of obtaining representative samples from shallow depths presumably influenced by biogeochemical process within the marsh rhizosphere and tidal pumping, 20 cm, and deeper processes presumably influenced by physical forces such as submarine estuary border and groundwater flow, 120 cm. Because this study measures pore water residence time to understand marsh drainage, the sampling locations were distributed from the marsh edge with a tidal channel, at about 0.5 m from the overlaying water in the tidal channel, toward the interior of the marsh, at about 60 m from the tidal channel.

**2.1. Pore water sampling:** Samples were collected using PushPoint samplers (MHE products 1/4" diameter PPX36 and PPX72 Field Investigation Sampler). A 150 ml syringe was connected to the PushPoint sampler to create the pressure for the flow of water and collect the sample. Once the sampler had been inserted into the sediments, the guard-rod was removed from the PushPoint to open its screen. Because a 150 ml syringe was used to collect 4 L samples, a pinch clamp was used to avoid the re-introduction of air and maintain the head on the sampling system. The clamp was pinched each time the syringe assembly was removed to dispense its contents. The samples were filtered in the field through a series of filters from 10 micron to 0.45 microns (QED disposable QuickFilters high-capacity in-line field filter) between the PushPoint sampler and the syringe (Figure 3). Once pore water starts flowing with no turbidity through the Push Point and high capacity filters, the flow rate was approximately  $0.5 \text{ L min}^{-1}$

**2.2. Sediment Sampling:** Sediment samples (~500 g/sample) were collected from each sampling station and depths (20 cm and 120 cm). The sediments for each depth were collected using a core sampler (Oakfield Model B Tube Sampler Soil Probe). The isolated samples were then put in plastic bags and immediately transported to the laboratory in a cooler. Once in the laboratory, each sample was put in a 250 ml beaker and oven dried at  $100 \text{ }^{\circ}\text{C}$  for a few days.

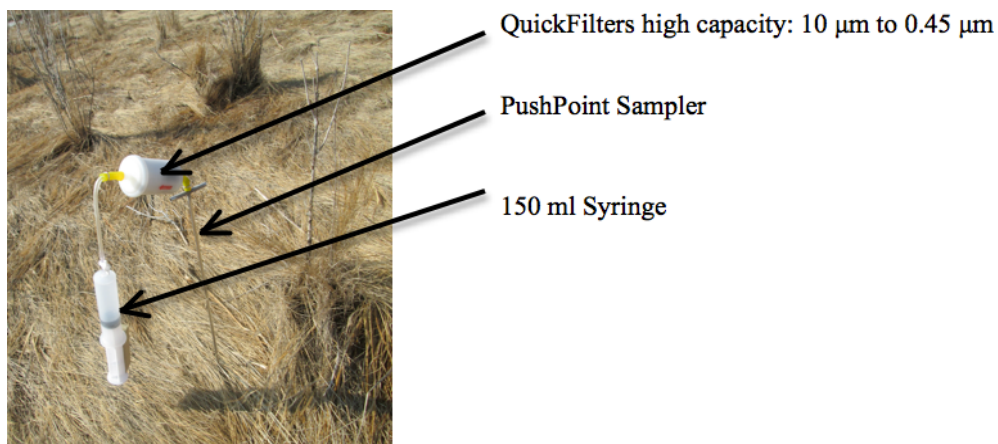


Figure 3. Pore water sampling using a PushPoint sampler, high capacity filter (1 to 0.5 microns) and a 150 ml syringe.

After the sediment samples were dry, they were sieved to eliminate loose organic fragments. Following sieving, each sample was ground using a coffee grinder and the dry weight was measured. Uranium and thorium series activities ( $^{226}\text{Ra}$ ,  $^{228}\text{Ra}$ ,  $^{228}\text{Th}$ ,  $^{238}\text{U}$ ) from sediment samples were determined using gamma-ray spectroscopy. Gamma-emitting daughters that were used for  $^{226}\text{Ra}$ ,  $^{228}\text{Ra}$ ,  $^{228}\text{Th}$ ,  $^{238}\text{U}$  include, respectively:  $^{214}\text{Pb}$  (352 keV),  $^{228}\text{Ac}$  (911 keV),  $^{208}\text{Tl}$  (593 keV), and  $^{234}\text{Th}$  (63 keV). Secular equilibrium was assumed between the daughter and parent in each case.  $^{235}\text{U}$  activities were calculated from the  $^{238}\text{U}$  activity using the average 238:235 atom ratio of 137.88. Approximately 20g from each sample from all marsh sites were enclosed in 20 mL polypropylene vials. The calculation from cpm to dpm was made using the detection efficiency for each of the radionuclides, determined by counting NIST Standard Reference Material 4350B. The  $^{234}\text{Th}$  activities were corrected for self-absorption by determining the transmission of a gamma source through the sample (T) and an empty container ( $T_0$ ) and by the  $T/T_0$  compared with a standardized core.

**2.2. Pore water sampling events:** Samples were collected from each marsh in July (summer) and November-December (early winter) of 2013 over a three-station transect from the inner marsh to the marsh bank adjacent to a tidal channel. All pore water samples were collected at mid-tide from low to high tide. In total, 42 samples of 4 L each were collected from the sampling locations; 2 per sampling station (one at 20 cm and one at 120 cm depth), with 3 sampling locations (6 samples) per marsh.

**2.3. Water quality parameters (temperature, salinity, and dissolved oxygen):** The water quality parameters were measured in the field using a YSI probe (YSI 85) immediately or during the collection of samples. The geographical coordinates for each sampling location were recorded with a GPS unit on all marshes and verified each time a sample was collected.

**2.4. Measurement of the short-lived radium isotopes ( $^{223}\text{Ra}$  and  $^{224}\text{Ra}$ ):** The extraction and quantification of Ra isotopes from the marsh pore water samples was conducted following the manganese dioxide  $\text{MnO}_2$ -impregnated acrylic fiber method using a Delayed Coincidence Counter (RaDeCC) system (Moore and Arnold, 1996; Garcia-Solsona et al., 2008).

The pore water samples collected and filtered in the field, at 20 cm and 120 cm depth for each station and along a transect of 3 stations for each of the three marshes, were stored in 4 L containers and taken to the laboratory the same day. Upon arrival of pore water samples to the laboratory, the volume was measured with a graduated cylinder and  $\text{MnO}_2$ -fibers were left overnight in the samples inside an Erlenmeyer flask. The  $\text{MnO}_2$ -fibers were then recovered, partially dried and placed in a RaDeCC system as described by Moore and Arnold (1996). Helium gas was circulated through the RaDeCC and over the Mn-fiber to sweep radon daughters of  $^{223}\text{Ra}$  and  $^{224}\text{Ra}$  ( $^{219}\text{Rn}$  and  $^{220}\text{Rn}$ , respectively) into a scintillation cell detector where the alpha decays of  $^{220}\text{Rn} - ^{216}\text{Po}$  and  $^{219}\text{Rn} - ^{215}\text{Po}$  pairs decay in the scintillation cell and then can be used to identify the radon isotope. The signals from the detector are routed to a delayed coincidence counter (RaDeCC). The alpha particles are recorded through a photomultiplier attached to the scintillation cell and the delayed coincidence circuit sorts signals generated by the decay of  $^{219}\text{Rn}$  to  $^{215}\text{Po}$  ( $T_{1/2} = 1.8$  ms) and  $^{220}\text{Rn}$  to  $^{216}\text{Po}$  ( $T_{1/2} = 150$  ms) (Garcia-Solsona et al., 2008).

**3. Results:** The data on Ra isotopes (dpm/100 L) and water quality parameters; temperature ( $^{\circ}\text{C}$ ), salinity (PSU), and dissolved oxygen (mg/L) are presented in Table 1.

### 3.1. Temperature

**3.1.1. Summer:** Wertheim 1 had an average temperature for the whole transect of  $25^{\circ}\text{C}$  for shallow (20 cm) samples and  $23^{\circ}\text{C}$  for deep (120 cm) samples. Shallow samples had higher temperatures through the transect with a maximum value of  $27.2^{\circ}\text{C}$  for the marsh edge shallow

sample and the lowest value for the marsh interior deep sample with 21°C. The temperature of the water in the tidal channel was 26°C. The results seem to show a pattern that applies for both shallow and deep samples, from higher temperatures at the marsh edge to lower temperatures toward the marsh interior (Fig. 4A).

Wertheim 2 had an average temperature of 25°C for shallow samples and 23°C for deep samples. The highest temperature was measured at the marsh edge shallow sample with 27°C and the lowest for the marsh interior deep sample with 19.2°C. The temperature of the water in the tidal channel was 27°C. The results seem to show a pattern for the transect from higher temperatures at the marsh edge to lower temperatures toward the interior, however higher temperatures were measured for the shallow samples (Fig. 4B).

As described above, there is a possible horizontal pattern for temperature at Wertheim 1 and 2, characterized by higher values at the marsh edge toward lower values toward the marsh interior. A similar observation was made for salinity values for the same marshes.

Seatuck had an average temperature of 26°C for both; shallow (20 cm) samples and deep (120 cm) samples. There were no clear differences between shallow and deep samples. The highest temperature was measured for the marsh interior with 26.9 °C for shallow and deep samples. The lowest temperature was measured at the marsh edge with 25.1°C – 25.2°C for shallow and deep samples. The temperature of the water in the tidal channel was 26°C. In comparison with the Wertheim marshes, Seatuck had the highest temperatures toward the marsh interior and no clear pattern was observed (Fig. 4C).

**3.1.2. Winter:** The average winter temperature for Wertheim 1 was 9°C for both shallow and deep samples. The highest temperature was at the marsh edge with 9.9°C and the lowest at the mid-marsh shallow sample with 8.5°C. The water temperature at the tidal channel was 8.5°C. The results show a possible pattern from higher temperatures at the marsh edge to lower temperatures toward the mid-marsh (Fig. 4A). The average temperature for Wertheim 2 was 17°C for both; shallow and deep samples. The higher temperatures were measured at the marsh edge with 17.4°C and 17.3°C for shallow and deep samples respectively. The water temperature at the tidal channel was 17°C. Shallow samples seemed to have a pattern of high to low salinity

values from the marsh edge with 17.4°C to 16.8°C toward the marsh interior, however the deep samples did not show clear differences from marsh edge to marsh interior (Fig. 4B).

Seatuck had an average winter temperature of 3°C for shallow (20 cm) samples and 5°C for deep (120 cm) samples. Shallow samples had lower temperatures than deep samples. The lowest measured temperature for Seatuck was at the marsh edge shallow with 2.9°C while the deep sample at the marsh edge was 4.5°C. The water temperature at the tidal channel was 3°C. There was no clear pattern for temperature values at Seatuck during winter, however deep samples presented higher temperatures than shallow samples throughout the transect (Fig. 4C).

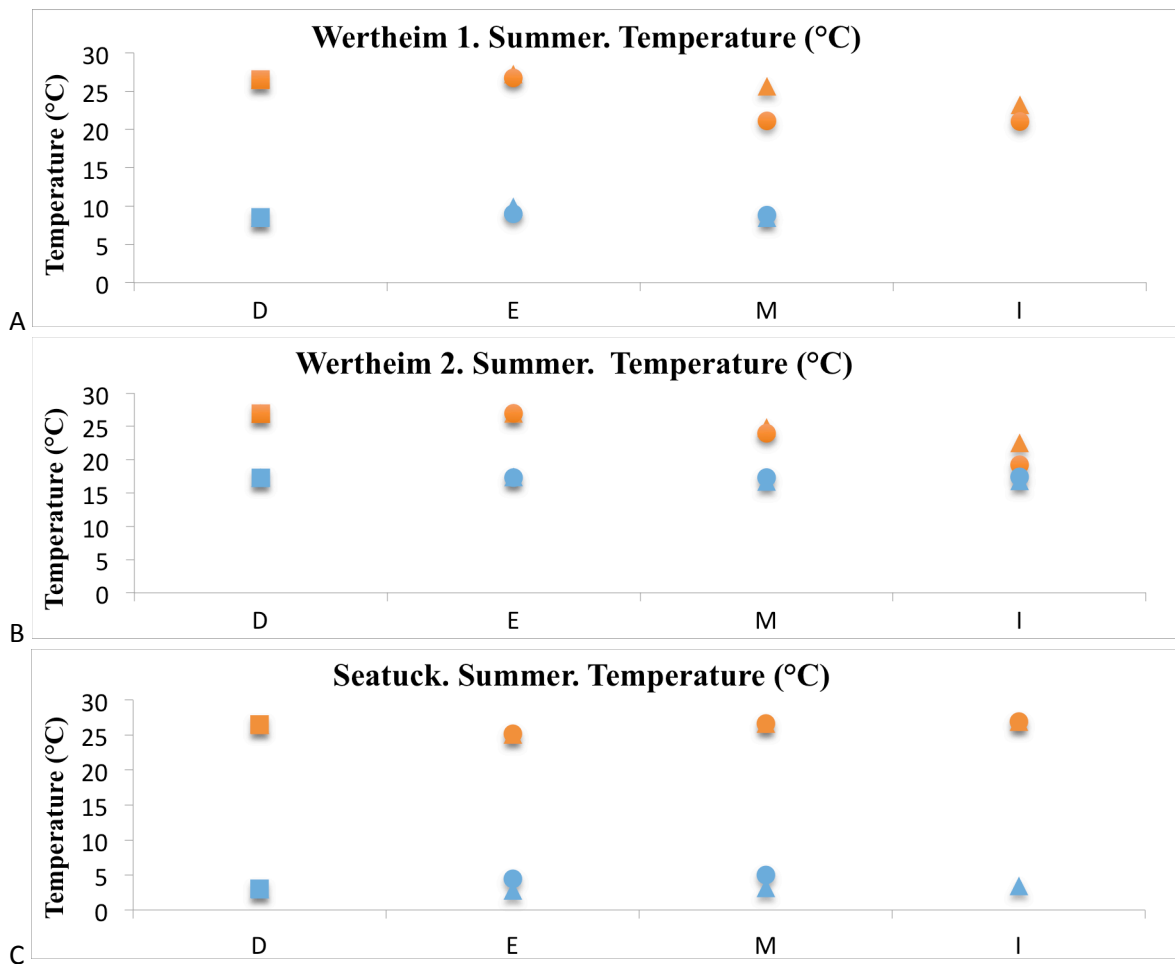


Figure 4. Temperature ( $^{\circ}\text{C}$ ) for all marshes, summer and winter. D: tidal ditch (channel), E: Marsh edge, M: Mid marsh, I: Marsh interior.  $\blacksquare$ : Summer tidal ditch water,  $\blacksquare$ : Summer tidal ditch water,  $\blacktriangle$ : 20 cm Summer,  $\bullet$ : 120 cm Summer,  $\blacktriangle$ : 20 cm Winter,  $\bullet$ : 120cm Winter.

**3.2. Radium:**  $^{223}$ ,  $^{224}$ Ra (dpm/100 L) in the pore water for all the marshes are given in Table 1. The data were corrected for cross-talk coincident counts, background counts, and efficiencies of RaDeCC detectors following Moore and Cai (2013) and Garcia-Solsona et al. (2008).

**3.2.1. Summer:** Wertheim 1 had an average  $^{224}$ Ra of 220 dpm/100L for shallow (20 cm) samples and 207 dpm/100L for deep (120 cm) samples (Fig. 5A). The lowest  $^{224}$ Ra activity was at the marsh edge shallow sample with 94.8 dpm/100L, while the opposite was found for deep samples with 276 dpm/100L. The average  $^{223}$ Ra activities were 15.8 dpm/100L and 8.2 dpm/100L for shallow and deep samples respectively, and the highest activities at the marsh interior with 20.2 dpm/100L and 11.9 dpm/100L for shallow and deep samples respectively (Fig. 5B).

For Wertheim 2, the  $^{224}$ Ra averages were 242 dpm/100L for shallow samples and 130 dpm/100L for deep samples (Fig. 5C), indicating a more significant difference between shallow and deep than on Wertheim 1. The highest  $^{224}$ Ra activities were found at the marsh edge for shallow (295 dpm/100L) and deep samples (244 dpm/100L). The average  $^{223}$ Ra activities for Wertheim 2 were 6.8 dpm/100L and 8.4 dpm/100L for shallow and deep samples respectively, and the highest activities were at the mid-marsh for shallow (8.2 dpm/100L) and at the marsh bank for deep (13.6 dpm/100L) samples (Fig. 5D).

The average  $^{224}$ Ra activities for Seatuck were 314 dpm/100L and 217 dpm/100L for shallow and deep samples respectively (Fig. 5E). The highest  $^{224}$ Ra activities were found at the marsh bank for both shallow (530 dpm/100L) and deep (258.1 dpm/100 L) samples. The average  $^{223}$ Ra activities were 13.4 dpm/100L and 12.1 dpm/100L for shallow and deep samples respectively. The highest  $^{223}$ Ra activities were also found at the marsh bank: 18.4 dpm/100L and 14.4 dpm/100L for shallow and deep samples respectively (Fig. 5F).

**3.2.2. Winter:** The average  $^{224}$ Ra activities for Wertheim 1 indicate higher Ra activities compared with Summer, with 351 dpm/100L and 427 dpm/100L for shallow and deep samples respectively. The highest activities were found at the mid-marsh site with 376 dpm/100L and 531 dpm/100L for shallow and deep samples respectively. The average for  $^{223}$ Ra was 18 dpm/100L and 14.5 dpm/100L for shallow and deep samples respectively and the highest activities were also found at the mid-marsh with 24.4 dpm/100L and 18.8 dpm/100L for shallow and deep samples respectively (Fig. 5A, B). The results for Wertheim 2 for  $^{224}$ Ra activities were

155 dpm/100L and 128 dpm/100L for shallow and deep samples respectively. The average  $^{223}\text{Ra}$  activities for Wertheim 2 were 4.0 dpm/100L and 3.1 dpm/100L for shallow and deep samples respectively, however the highest activities were found at the marsh edge for deep samples with 4.3 dpm/100L an at the marsh interior for shallow samples with 7.3 dpm/100L (Fig. 5C, D).

The winter results for Seatuck indicated average  $^{224}\text{Ra}$  activities of 369 dpm/100L and 346 dpm/100L for shallow and deep samples respectively. The highest  $^{224}\text{Ra}$  activities were found at the marsh bank with 431.5 dpm/100L and 400.8 dpm/100L for shallow and deep samples. The average activities for  $^{223}\text{Ra}$  were found at 20 dpm/100L and 16 dpm/100L for shallow and deep samples respectively and the highest activities were also found at the marsh bank with 20.5 dpm/100L and 16.4 dpm/100L for shallow and deep samples respectively (figure 5E, F).

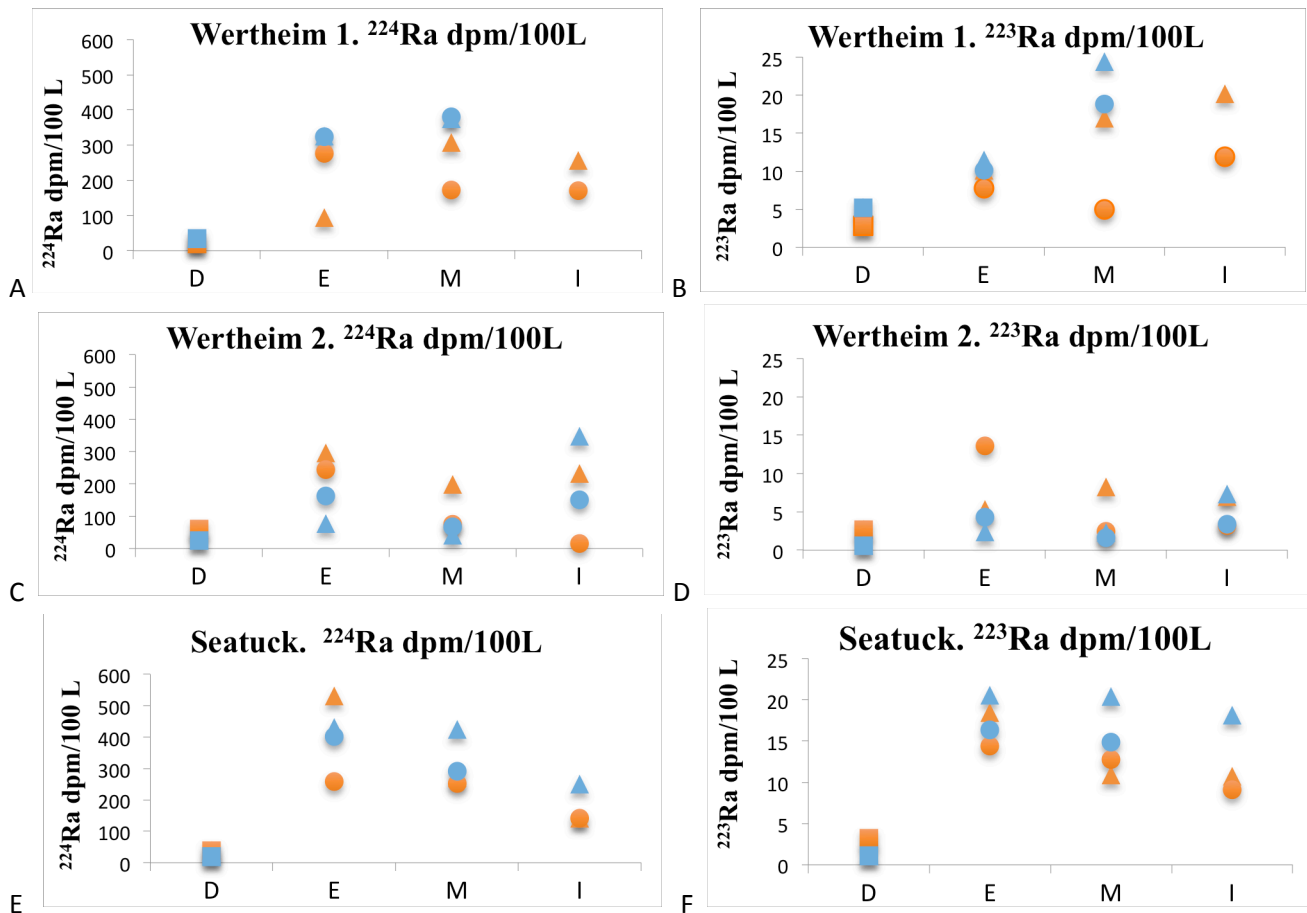


Figure 5.  $^{224}\text{Ra}$  and  $^{223}\text{Ra}$  (dpm) activities for summer. D: tidal ditch (channel), E: Marsh edge, M: Mid marsh, I: Marsh interior. ■: Summer tidal ditch water, ■: Summer tidal ditch water, ▲: 20 cm Summer, ●: 120 cm Summer, ▲: 20 cm Winter, ●: 120cm Winter.



### 3.3. Salinity

**3.3.1. Summer:** Wertheim 1 had an average salinity (PSU) for the whole transect of 13 for shallow (20 cm) samples and 16 for deep (120 cm) samples. Deep samples had higher salinities than shallow samples. The lowest measured salinities were at the marsh interior with 11.2 ‰ and 14.8 for shallow and deep samples respectively. The highest measured salinities were at the marsh edge with 14.7 and 17.9 for shallow and deep samples respectively, and the water salinity of the tidal channel was 8.1 (Fig. 6A).

The average salinity for Wertheim 2 was 13 for shallow samples and 12 for deep samples. Averages between shallow and deep samples was similar, however deep samples had a bigger amplitude from the highest at the marsh edge with 19 to the lowest at marsh interior with 6 while for shallow samples the highest value was also at marsh interior with 15.7 and the lowest also at the marsh interior with 11.5. The water salinity in the tidal channel was 8.4 (Fig. 6B). Salinity values for Wertheim 1 and 2 seemed to have a spatial horizontal pattern characterized by higher values at the marsh edge to lower values toward the marsh interior.

Seatuck had an average salinity for the whole transect of 22 for shallow (20 cm) samples and 15 for deep (120 cm) samples. Shallow samples had higher salinities than deep samples. The lowest salinities were at the marsh interior with 21.7 and 12.5 for shallow and deep samples respectively. The highest measured salinities were at the mid-marsh with 22.3 and 16.3 for shallow and deep samples respectively. The water salinity in the tidal channel was 20.5. As a difference with the Wertheim marshes, Seatuck had the highest salinities in the mid-marsh and the spatial pattern seemed to be vertical with higher salinities found on shallow samples and lower values for deep samples (Fig. 6C).

**3.3.2. Winter:** In general, winter samples had higher salinity values than summer samples. Wertheim 1 had an average salinity for the whole transect of 14 for shallow (20 cm) samples and 17 for deep (120 cm) samples. The lowest measured salinities were at the marsh edge with 12.5 and 16 for shallow and deep samples respectively. The highest salinities were at the mid-marsh with 14.5 and 17.5 for shallow and deep samples respectively, and the water salinity in the tidal channel was 8.7 (Fig. 6A).

The average salinity for Wertheim 2 was 28 for shallow samples and 22 for deep samples.

Shallow samples were characterized by a spatial pattern of high to low salinity values from the marsh edge with 30.4 to the marsh interior with 25.6. Deep samples did not have significant spatial differences with the marsh edge with 21.6, mid-marsh with 21.3, and the marsh interior with 21.9. The water salinity in the tidal channel was 15.2 (Fig. 6B).

Seatuck had an average salinity for the whole transect of 24 for shallow (20 cm) samples and 16 for deep (120 cm) samples. Shallow samples had higher salinities than deep samples. The lowest measured salinities were at the marsh interior with 21.6 for the shallow sample and at the mid-marsh with 13 for the deep sample. The highest measured salinities were at the mid-marsh with 25.8 for the shallow sample and 19.4 for the deep sample. The water salinity in the tidal channel was 21.36 The shallow samples presented higher salinities than the deep samples, indicating that the same vertical pattern from summer was characterizing salinity in winter (Fig. 6C)

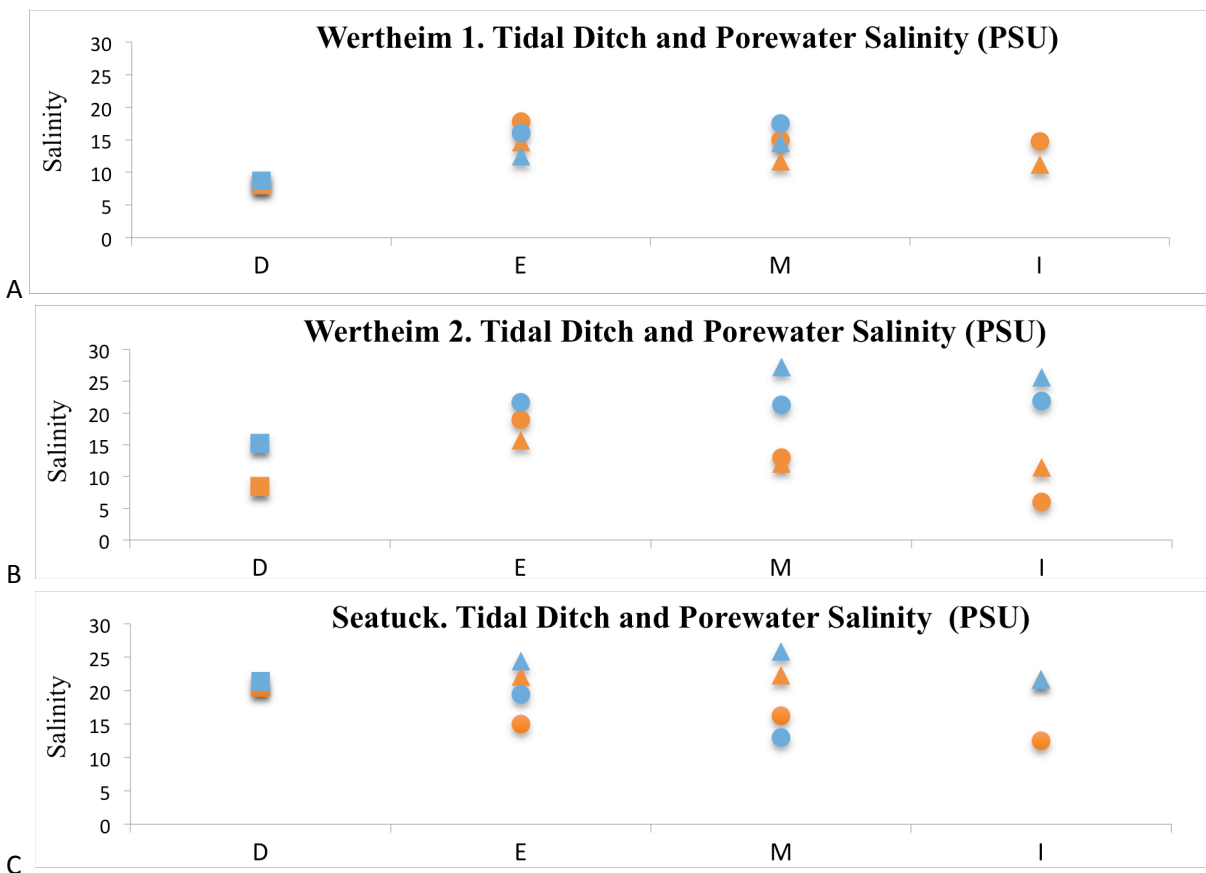


Figure 6. Tidal ditch and pore water salinity values (‰) for summer and winter. D: tidal ditch (channel), E: Marsh edge, M: Mid marsh, I: Marsh interior. ■: Summer tidal ditch water, ■: Summer tidal ditch water, ▲: 20 cm Summer, ●: 120 cm Summer, ▲: 20 cm Winter, ●: 120cm Winter.

**3.3.3. Radium Isotopes versus Salinity:** Figure 7 shows the activities for  $^{224}\text{Ra}$  and  $^{223}\text{Ra}$  versus salinity for all marshes. Wertheim 1 shows a possible vertical pattern for summer, with high Ra activities (dpm/100 L) at shallow samples (20cm) and low salinities, while deep samples (120 cm) showed lower Ra activities and higher salinity values (Fig. 7A). Winter samples also showed lower salinities for shallow samples and higher salinities for deep samples, however there was no clear pattern for Ra activities, although the averages for both;  $^{224}\text{Ra}$  and  $^{223}\text{Ra}$  were higher on winter than summer (Fig. 7B).

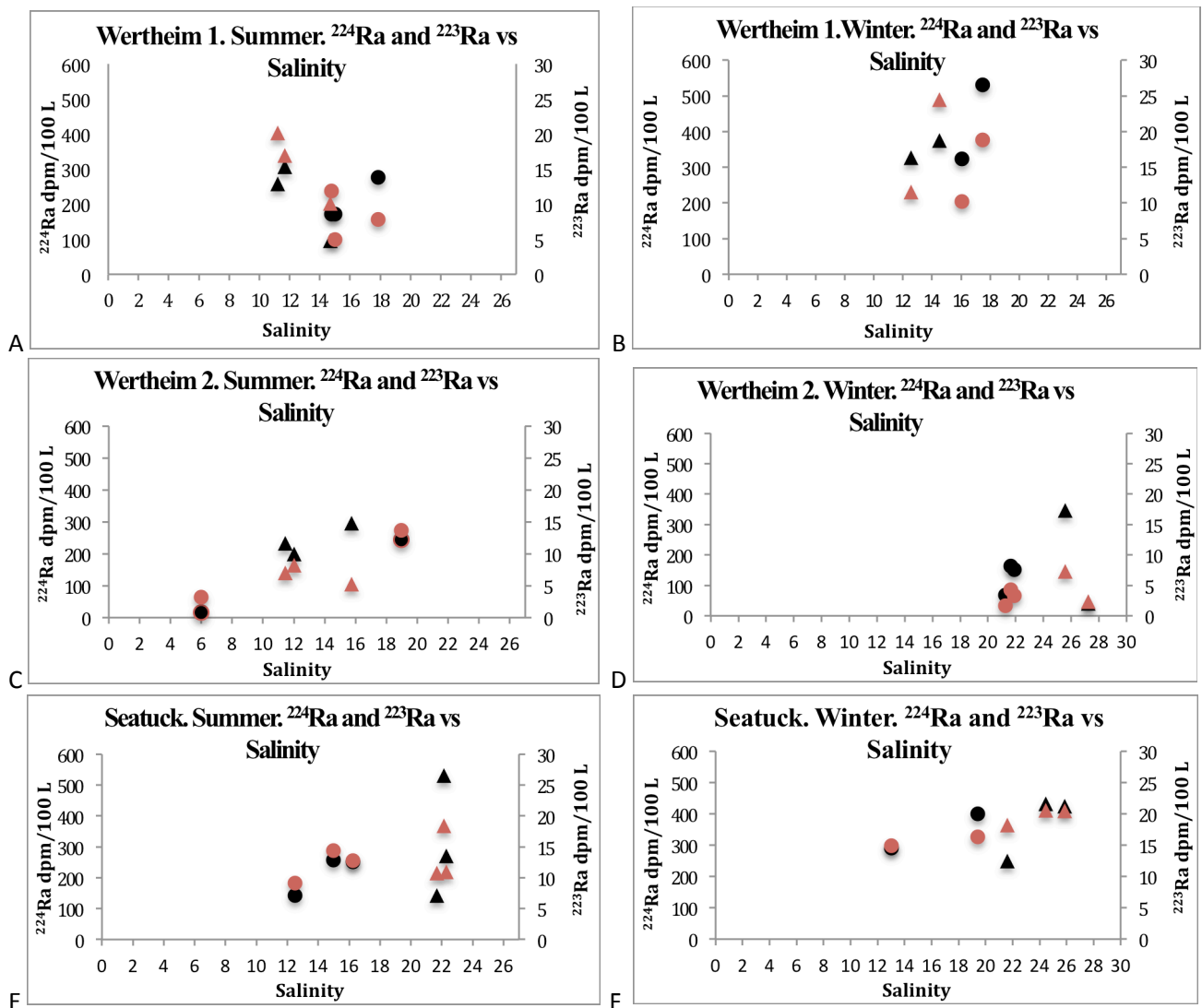


Figure 7.  $^{224}\text{Ra}$  and  $^{223}\text{Ra}$  activities (dpm/100 L) versus salinity (PSU) for summer and winter samples. Series symbols:  $\blacktriangle$ : 20 cm  $^{224}\text{Ra}$ ,  $\bullet$ : 120cm  $^{224}\text{Ra}$ ,  $\blacktriangle$ : 20cm  $^{223}\text{Ra}$ ,  $\bullet$ : 120cm  $^{223}\text{Ra}$ .

The results for summer for Wertheim 2 show increasing Ra activities with increasing salinities. However, Ra activities from shallow samples were grouped within a salinity range of 11.5 to 15.7, and deep samples had two groups; the first with low Ra activities and low salinity (~6) and the second with higher Ra activities and high salinity 19 (Fig. 6C). The Wertheim 2 Ra activities at 120 cm for winter were grouped within 21 and 22, while 20 cm samples showed Ra activities at higher salinities within 25.6 to 27.2 (Fig. 7D).

There seems to be a correlation between Ra activities and salinity for Seatuck for both; summer and winter. However shallow samples had higher salinities and Ra activities for (Fig. 7E, F), and winter samples seem to group shallow samples within higher salinities than deep samples.

### **3.4. Dissolved Oxygen**

**3.4.1. Summer:** Dissolved oxygen (DO) was not measured for Wertheim 1 due to field problems with the DO YSI probe, as described in the methods section. The average DO (mg/L) for Wertheim 2 was 3 mg/L for shallow samples and 4 mg/L for deep samples. The DO for deep samples were higher than the DO for shallow samples, however the highest DO was measured at the mid-marsh shallow sample with 5.6 mg/L. The lowest DO was measured at the marsh edge shallow sample with 1.5 mg/L (Fig. 8B). DO for Wertheim 1 and 2 seemed to have a horizontal pattern with higher values at the marsh edge to lower values toward the marsh interior.

The average DO values for Seatuck were 2 mg/L and 1 mg/L for shallow and deep samples respectively. Although shallow samples had a higher DO, the difference between shallow and deep samples was not significant. The highest DO value was measured at the mid-marsh shallow sample with 1.7 mg/L and the lowest at marsh interior, ~1.2 mg/L and ~1.2 mg/L at shallow and deep samples. Although there was no clear pattern, the tendency for deep samples was from high to low DO from the marsh edge to the interior (Fig. 8C).

**3.4.2. Winter:** The average DO for Wertheim 1 was 5 mg/L for both; shallow and deep samples. The average and specific DO values were similar for shallow and deep samples, although there seems to be a tendency for shallow samples to go from low DO at the marsh edge to higher DO at the mid-marsh. The opposite was seen for deep samples (Fig 8A).

The average DO for Wertheim 2 was ~1.0 mg/L for both; shallow and deep samples. The highest DO value was measured at the marsh edge shallow sample with 2.1 mg/L and the lowest at the mid-marsh deep sample with 0.8 mg/L. The measured DO does seem to show significant differences between shallow and deep samples. However the difference between shallow and deep samples at the marsh edge was from 2.1 mg/L to 0.8 mg/L for shallow and deep samples respectively, which was more noticeable than the other sampling stations (Fig. 8B).

Seatuck had an average DO of 6 mg/L for shallow samples and 5 mg/L for deep samples. The highest DO value were measured at the marsh edge and mid-marsh shallow samples with 6 mg/L and the lowest values were at the marsh edge deep sample with 4 mg/L. Shallow samples had higher DO values than deep samples (Fig. 8C).

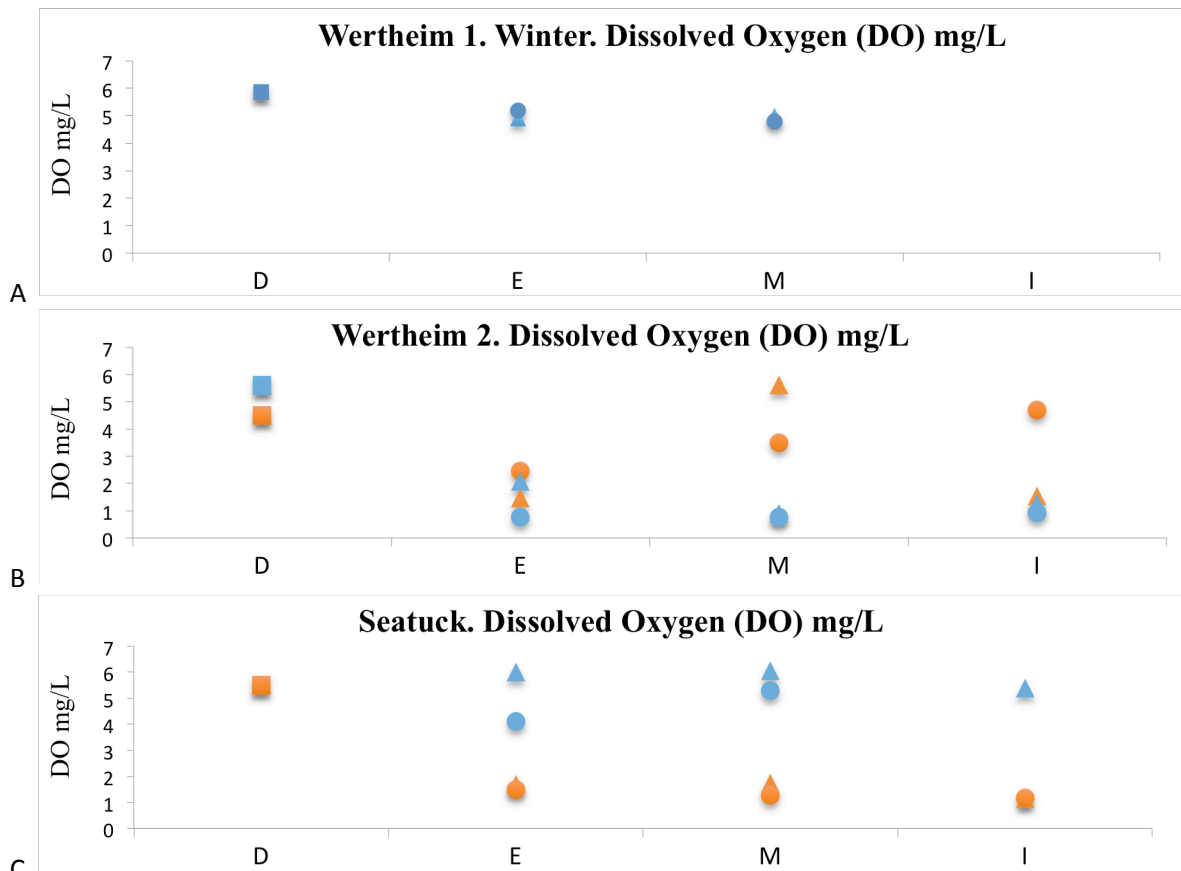


Figure 8. Dissolved oxygen (DO) for summer and winter. D: tidal ditch (channel), E: Marsh edge, M: Mid marsh, I: Marsh interior. ■: Summer tidal ditch water, ■: Winter tidal ditch water, ▲: 20 cm Summer, ●: 120 cm Summer, ▲: 20 cm Winter, ●: 120cm Winter.

**3.4.3. Radium Isotopes versus Dissolved Oxygen:** Figure 9 shows the activities for  $^{224}\text{Ra}$  and  $^{223}\text{Ra}$  (dpm/100 L) versus dissolved oxygen (mg/L) for all marshes. The results do not show significant spatial or temporal patterns between dissolved oxygen and Ra activities.

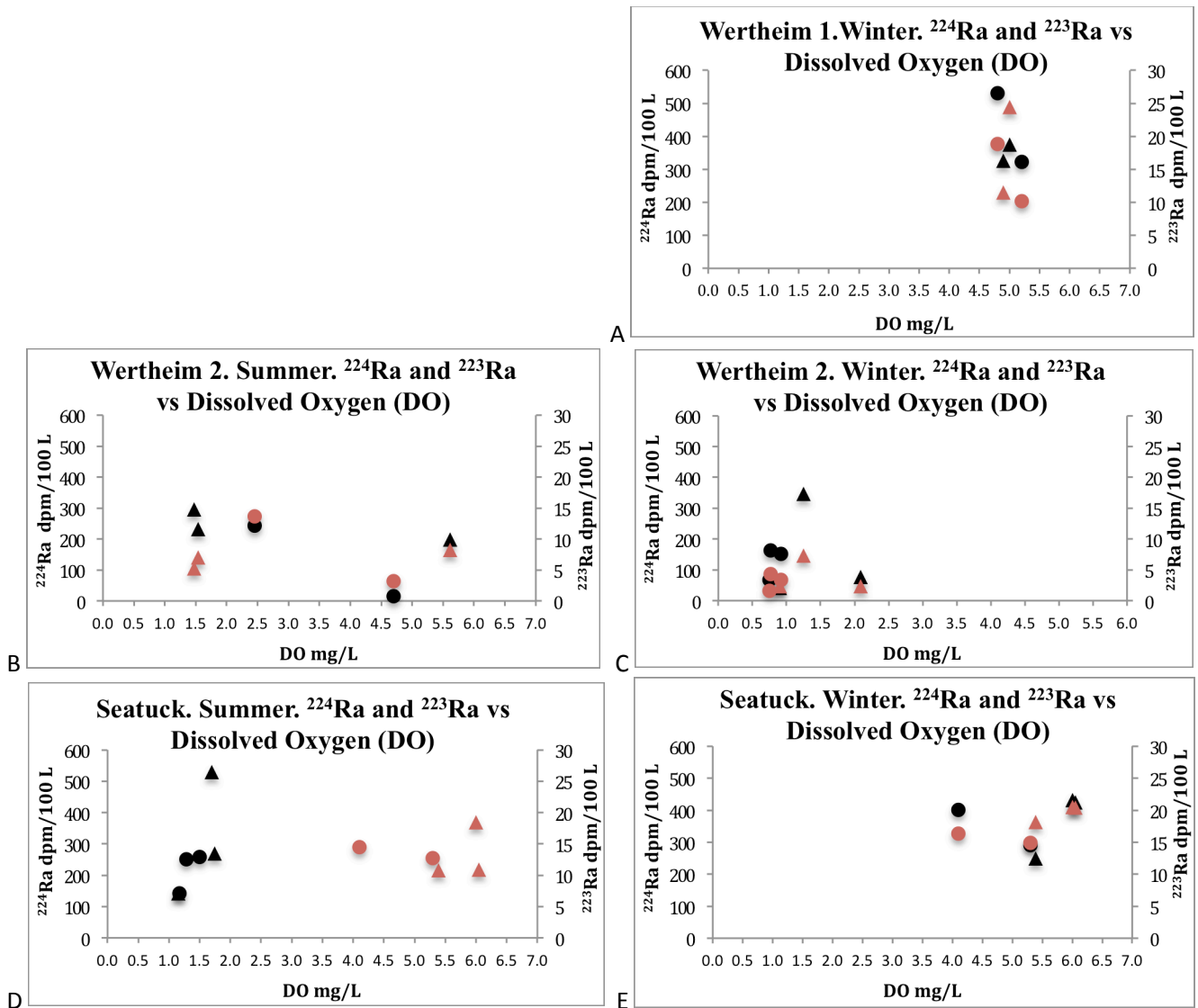


Figure 9. Radium isotopes ( $^{224}\text{Ra}$  and  $^{223}\text{Ra}$ ) versus dissolved oxygen for summer and winter samples. Series symbols:  $\blacktriangle$ : 20 cm  $^{224}\text{Ra}$ ,  $\bullet$ : 120cm  $^{224}\text{Ra}$ ,  $\blacktriangle$ : 20cm  $^{223}\text{Ra}$ ,  $\bullet$ : 120cm  $^{223}\text{Ra}$ .

**3.5. Solid phase radionuclide data:** The solid phase activities for radionuclides  $^{226}\text{Ra}$ ,  $^{228}\text{Ra}$ ,  $^{228}\text{Th}$ , and  $^{235}\text{U}$ , in dpm/g were determined for each sediment sample at each station and depth for all marshes (Table 2). We focused on the activities of  $^{228}\text{Th}$  and  $^{238}\text{U}$  ( $^{235}\text{U}$ ) because these

serve as source radionuclides for  $^{224}\text{Ra}$  and  $^{223}\text{Ra}$ , respectively. The results for  $^{228}\text{Th}$  activities for Wertheim show values of 1.3 dpm/g for shallow (20 cm) and 1.1 dpm/g for deep (120 cm) samples at the marsh edge. The values for the mid-marsh were 0.9 dpm/g for both; shallow (20 cm) and deep (120 cm) samples. These results show a decreasing pattern from marsh edge to the mid-marsh (Fig. 10A). Wertheim 2 shows a similar decreasing pattern from marsh edge to mid-marsh with an average of  $\sim 0.6$  dpm/g for the marsh edge to 0.9 for the mid-marsh (Fig. 10A). The results for  $^{228}\text{Th}$  for Setauck were more equally distributed through the marsh with 1 dpm/g and 0.8 dpm/g for shallow and deep samples respectively at the marsh edge and 0.9 for both; shallow and deep samples at the marsh mid-marsh (Fig 10A). Organic matter as diverse vegetation pieces and roots attached to marsh vegetation were found on sediment samples from 20 cm depth for all marshes as evidence that the 20 cm depth is within the rhizosphere zone, while samples for 120 cm depth were mostly sediments with no differentiable organic matter.

The results for  $^{235}\text{U}$  for Wertheim 1 show an average of  $\sim 0.28$  dpm/g for both; shallow (20 cm) and deep (120 cm) samples at the marsh edge and an average of  $\sim 0.21$  dpm/g for both; shallow and deep samples at the mid-marsh (Fig. 10B). The results show a horizontal decreasing pattern from marsh edge to marsh interior. The results for Wertheim 2 show an increasing pattern from the marsh edge ( $\sim 0.16$  dpm/g) to the mid-marsh ( $\sim 0.20$  dpm/g) (Fig. 10B). Setauck appears to present a vertical distributions of  $^{235}\text{U}$  from high (0.25 dpm/g) at the marsh edge shallow samples to low (0.07 dpm/g) at the marsh edge deep samples, and from low (0.25 dpm/g) at the mid marsh shallow samples to high (1.2 dpm/g) at the mid-marsh deep samples (Fig. 10B).

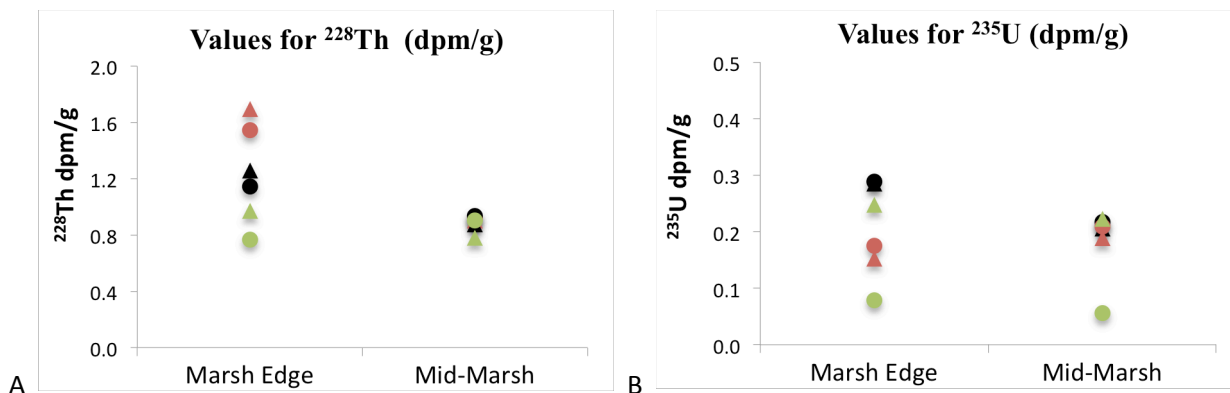


Figure 10.  $^{228}\text{Th}$  and  $^{235}\text{U}$  activities (dpm/g) for all marshes versus sampling stations. ▲: 20 cm Wertheim 1, ●: 120 cm Wertheim 1, ▲: 20 cm Wertheim 2, ●: 120 cm Wertheim 2, ▲: 20 cm Setauck, ●: 120 cm Setauck

The uranium ( $^{238,235}\text{U}$ ) activities for the Wertheim and Seatuck shallow samples were high relative to the other samples. Church et al. (1996) showed that marshes are strong sinks for uranium and this likely explains the high activities. The results for  $^{226}\text{Ra}$  and  $^{228}\text{Ra}$ , for Wertheim 1 showed decreasing activities from the marsh edge toward the mid-marsh (Fig 11A, B). The results for Wertheim 2 show a decreasing distribution of  $^{226}\text{Ra}$  from marsh edge to mid-marsh, and  $^{228}\text{Ra}$  also decreasing at shallow samples from the marsh edge to the mid-marsh, while the deep samples show an increasing distribution from the marsh edge to the mid-marsh (Fig 11A, B). The results for Seatuck did not show a clear vertical or horizontal distribution (Fig. 11A, B)

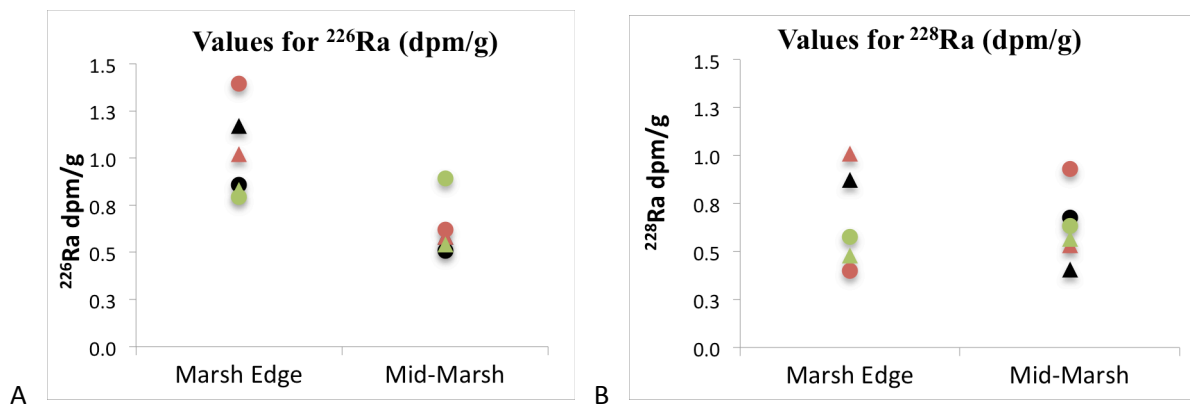


Figure 11. Activities for  $^{226,228}\text{Ra}$  from sediment samples for all marshes. ▲: 20 cm Wertheim , ●: 120 cm Wertheim 1, ▲: 20 cm Wertheim 2, ●: 120 cm Wertheim 2, ▲: 20 cm Seatuck , ●: 120 cm Seatuck

## 4. Discussion

**4.1. Estimating residence times of marsh pore water using  $^{224,223}\text{Ra}$ :** The short-lived Ra isotopes are introduced into the marsh pore water by recoil following their production from radioactive decay of their parents. Thus activity of radium in the pore water must reflect the length of time the pore water remains in contact with the solids. We have applied a simple one-dimensional model that has been used to characterize advective transport of radionuclides in groundwater (Krest and Harvey, 2003). Neglecting hydrodynamic dispersion,



$$\frac{\partial C_{Ra}}{\partial t} = -v \frac{\partial C_{Ra}}{\partial x} + \frac{P}{(1+K)} - \lambda C_{Ra} \quad [1]$$

where  $C_{Ra}$  is the concentration of dissolved Ra (atoms/volume of pore fluid),  $v$  is the pore water advective flow velocity (length/time),  $P$  is the rate of supply of Ra atoms to the fluid phase,  $\lambda$  is the Ra decay constant (1/time),  $K$  is a dimensionless sorption constant (dpm Ra on the solid/dpm Ra in solution) and  $x$  is distance along the fluid flow path.

Assuming steady-state ( $\partial C_{Ra}/\partial t = 0$ ), eqn 1 can be solved as:

$$C_{Ra} = P'\lambda^{-1} + (C_{Ra}^0 - P'\lambda^{-1})e^{-\frac{\lambda x}{v}} \quad [2]$$

where  $C_{Ra}^0$  is an initial Ra concentration in the fluid,  $P' = P/(1+K)$ . Multiplying through by  $\lambda_{Ra}$  converts the atom concentrations to activities (dpm/volume):

$$A_{Ra} = P' \left( 1 - e^{-\frac{\lambda x}{v}} \right) + A_{Ra}^0 e^{-\frac{\lambda x}{v}} \quad [3]$$

Krest and Harvey (2003) applied eqn 3 to detailed depth profiles of dissolved Ra in a freshwater wetland (the Florida Everglades) in which flow was dominantly vertical. In the present case, we have sampled the marsh pore water at only two depths and cannot assume that flow is predominantly vertical through the marsh. Indeed, the salinity measurements often show different salinities at 20 cm and at 120 cm, suggesting that lateral flow, perhaps involving fresher groundwater, may be occurring. Moreover there is no clear spatial variation in  $^{224}\text{Ra}$  such that the marsh edge is consistently different from mid-marsh and interior sites. This makes it difficult to ascertain a possible value of  $A_{Ra}^0$ . Thus we further simplify eqn 3, by assuming that  $A_{Ra}^0 = 0$ . Other possible sources of Ra, such as the tidal channels, have Ra activities significantly lower than those found in marsh pore water (Table 1). The Ra activities detected for the tidal channels for all marshes were between 19.2 dpm and 0.1 dpm for  $^{224}\text{Ra}$  and 2.8 dpm and  $^{223}\text{Ra}$ , which are comparable to  $^{224}, ^{223}\text{Ra}$  activities reported by Beck et al. (2008) for the Carmans River. The fraction of Ra from fresh groundwater was not determined during this study, and each parcel of

water sampled is assumed to be in balance with respect to sources of Ra and loss due to decay and flow out of the system.

Moreover, we do not have sufficient spatial data of Ra activities along possible flow paths of water in the marsh to apply eqn. 3 directly. Thus we convert eqn. 3 to a residence time formulation in which  $x/v$  is replaced by the parameter  $\tau$ :

$$A_{Ra} = P'(1 - e^{-\lambda\tau}) \quad [4]$$

Eqn. 4 treats the dissolved Ra in every parcel of water sampled as representing a balance between supply of Ra to the pore water and loss by decay and advection.

**4.1.1. Supply of  $^{224,223}\text{Ra}$  to marsh pore water:** Evaluating the term  $P'$  in eqn 4 is crucial to the calculation of marsh pore water residence times. The short-lived radium isotopes  $^{223}\text{Ra}$  and  $^{224}\text{Ra}$  enter sediment pore water principally through recoil after their production from decay of their parent nuclides,  $^{227}\text{Th}$  and  $^{228}\text{Th}$ , in the solid phase. Once in the pore water, their dissolved activities are controlled by radioactive decay, sorption onto the solid surfaces and any loss due to advection. The production of dissolved Ra is given by (Porcelli, 2008):

$$P' = \frac{b\varepsilon A_P}{1 + K} (10^5) \quad [5]$$

where  $P'$  = production rate (atoms/time/100L),  $b$  = g dry sediment/cm<sup>3</sup> pore water,  $\varepsilon$  = fraction of newly produced Ra atoms that are recoiled to pore water,  $A_P$  = solid phase parent ( $^{228}\text{Th}$  or  $^{227}\text{Th}$ ) activity (dpm/g) and  $K$  = dimensionless sorption constant of Ra ([dpm adsorbed Ra]/[dpm dissolved Ra]). The factor  $10^5$  converts the units from cm<sup>3</sup> to 100L to facilitate comparison with the units used for the dissolved  $^{223,224}\text{Ra}$  activities in Table 1. The term  $b$  is equivalent to the rock:water ratio used in modeling Ra isotopes in aquifers (Porcelli, 2008) and is calculated from the sediment porosity and densities of the solid and aqueous phases as:

$$b = \frac{(1 - \Phi)\rho_{sed}}{\Phi} \quad [6]$$

where  $\Phi$  = porosity ( $\text{cm}^3$  water/ $\text{cm}^3$  wet sediment) and  $\rho_{sed}$  = solid phase density ( $\text{g}_{sed}/\text{cm}^3_{sed}$ ). Porosity is determined from:

$$\Phi = \frac{W/\rho_w}{W/\rho_w + (1 - W)/\rho_{sed}} \quad [7]$$

where  $W$  = water content (g water/g wet sediment),  $\rho_{sed}$  and  $\rho_w$  are the densities of the solid and aqueous phases, respectively.

Marsh peat contains both organic matter and lithogenic sediment. The former is commonly high. For example at Wertheim marsh sites studied by Kolker et al. (2009), water content was 78-88% and organic matter based on loss-on-ignition was ~20-80%, with higher values in the upper 30-60 cm. The solid fraction marsh peat comprises lithogenic sediment and organic matter, and the appropriate value of  $\rho_{sed}$  to use in eqns. 6 and 7 is obtained from (Kolker et al., 2009):

$$\rho_{sed} = (1 - LOI)\rho_{lith} + (LOI)\rho_{om} \quad [8]$$

where LOI is the fractional organic content (g organic matter/g wet sediment),  $\rho_{lith}$  and  $\rho_{om}$  are the densities of lithogenic sediment and organic matter, assumed to be 2.6 and 1.2  $\text{g}/\text{cm}^3$ , respectively. For LOI values of 60%,  $\rho_{sed}$  is ~1.8. Similarly, for water contents of ~85%, porosity is 0.9. The parameter  $b$  is then ~0.2  $\text{g}_{sed}/\text{cm}^3$  water.

Applying eqn 5 to the Wertheim and Seatuck marsh sites also requires estimates of  $\epsilon$ ,  $K$ , and parent activities. We have measured the parent of  $^{224}\text{Ra}$ ,  $^{228}\text{Th}$ , in the sediment (Table 2), and activities range from 0.77 to 1.69 dpm/g.  $^{223}\text{Ra}$  is a member of the  $^{235}\text{U}$  decay series and its immediate parent is  $^{227}\text{Th}$ . This Th isotope is typically in equilibrium with its parent  $^{227}\text{Ac}$  (Griffin, 2011). In lithogenic sediment, the precursors of  $^{223}\text{Ra}$  in the  $^{235}\text{U}$  decay series are likely in radioactive equilibrium. As noted above, we have calculated the  $^{235}\text{U}$  activities from the measured  $^{238}\text{U}$  activities using the atom abundance ratio of  $^{238}\text{U}$  to  $^{235}\text{U}$  (137.88). In the present case, we use the  $^{234}\text{Th}$  activity as a measure of the  $^{238}\text{U}$  activity. All samples were counted sufficiently long after collection that  $^{234}\text{Th}$  was in equilibrium with  $^{238}\text{U}$ . The values of  $^{235}\text{U}$

calculated in this way range from 0.06 to 0.29 dpm/g. One difficulty with this method of estimating the  $^{227}\text{Th}$  activity is that U has been shown to be scavenged from solution onto marsh sediments, presumably as a result of redox processes operating in the marsh peat (Church, 1996). Indeed the  $^{238}\text{U}$  ( $^{234}\text{Th}$ ) activities are notably higher than the other  $^{238}\text{U}$  series radionuclide measured ( $^{226}\text{Ra}$ ), although preferential Ra mobilization from sediments is common. Because we are unable to ascertain the nature of enhanced U removal onto the marsh peat and the time scale, we used the  $^{235}\text{U}$  calculated from the  $^{238}\text{U}$  activities as an estimate of the parent ( $^{227}\text{Th}$ ) activity of  $^{223}\text{Ra}$  (Table 2).

Numerous studies have evaluated the recoil efficiency of Ra atoms to pore fluids. This parameter is critically dependent on grain size, with the higher surface area of smaller grain sizes promoting a larger fraction of nascent atoms recoiled to the pore water. Values of  $\epsilon$  have been estimated from the concentrations of  $^{222}\text{Rn}$  in pore fluids. This radionuclide is appropriate for this purpose because it is chemically unreactive once introduced to the pore fluid. Values of  $\epsilon$  have been estimated for the muddy sediments of Long Island Sound (LIS) (~30%; Cochran, 1979) and in the Upper Glacial Aquifer of Long Island (~3-5%; Copenhagen et al., 1993). Here we use an intermediate value, 10%, with the assumption that the grain size in the marsh peat is intermediate between that of LIS sediments and the Upper Glacial Aquifer.

The final parameter needed to apply eqn. 5 is the distribution coefficient of Ra in the marsh sediments. As defined in eqn. 5, this is a dimensionless quantity. A similar measure is  $K_D$ , (distribution coefficient) which is defined as  $[(\text{dpm Ra/g sed})/(\text{dpm Ra/cm}^3 \text{ water})]$ . In sediment systems,  $K_D = K/b$ , where K and b are as defined in eqn. 1. There is considerable variation in  $K_D$ , with values ranging from  $10$ - $10^2$  in the muddy sediments of Long Island Sound (Cochran, 1979) to  $10^3$  in deep-sea red clay sediments (Cochran and Krishnaswami, 1980). Values in Long Island and Connecticut aquifers are on the order  $10^2$ .  $K_D$  is dependent in the ionic strength of the fluid, with lower values in seawater compared with fresh water. Additionally, both grain size and redox conditions (e.g. presence of Mn oxides) can affect K. Rama and Moore (1996) determined  $K_D$  in a South Carolina salt marsh and found low values (~10) that they attributed to the elevated organic content of the marsh peat. For our purposes, we assume that the calculated value of  $P$  must be sufficiently large to produce the highest  $^{224}\text{Ra}$  activity observed in the marsh pore waters. This is ~530 dpm/100 L at both the Wertheim and Seatuck sites. Using a value of K of 4

for Wertheim and 3 for Seatuck in eqn 5 produces values of  $P$  that are  $\sim 530$  dpm/100L on average (Table 2). A slightly lower value of  $K$  for Seatuck is also justified because of the somewhat greater pore fluid salinities there, on average (Table 1). The values of  $K$  used here are equivalent to  $K_D$  values of 15-20 and thus are comparable to values determined in the salt mash studied by Rama and Moore (1996). Values of  $P$  for  $^{223}\text{Ra}$  are calculated from those of  $^{224}\text{Ra}$  by dividing by the solid phase  $^{228}\text{Th}/^{227}\text{Th}$  ( $^{235}\text{U}$ ) activity ratio (Table 2).

The increases in the activities of  $^{224}\text{Ra}$  and  $^{223}\text{Ra}$  as a function of residence time at the three marshes (eqn. 4) are shown schematically in Fig. 12. The different half-lives produce different time scales for the approach to a steady-state pore water activity.

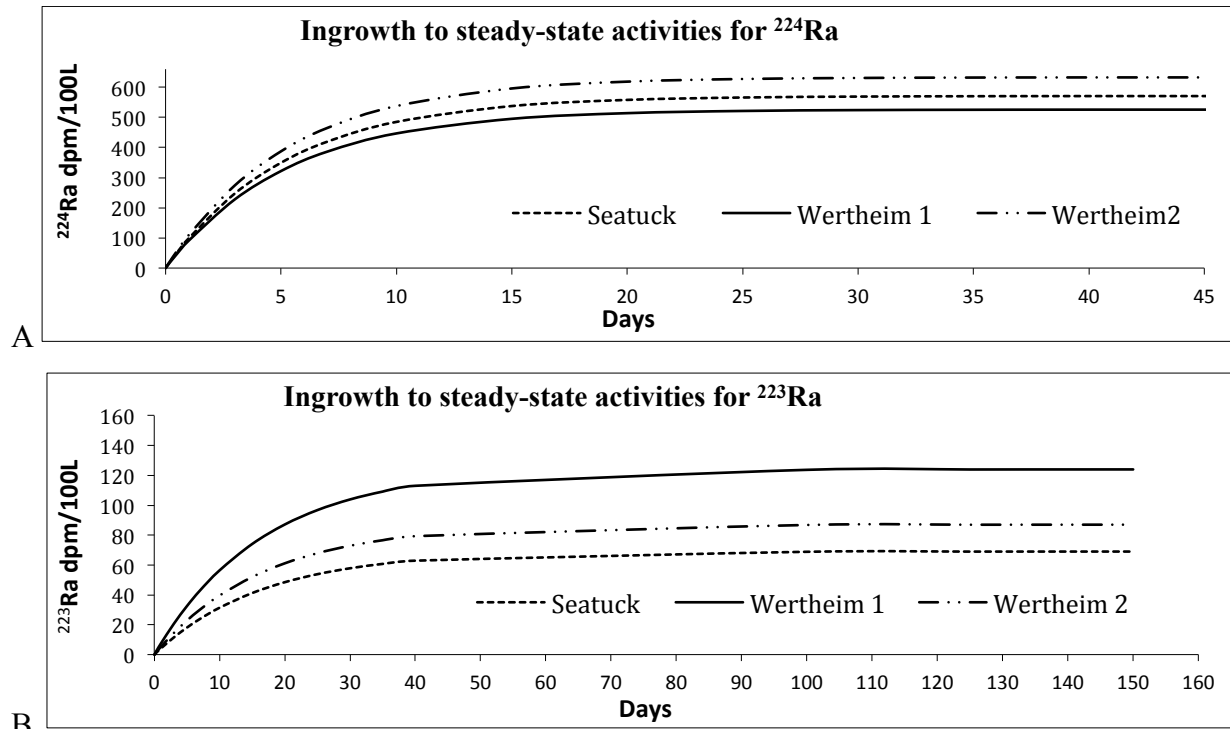


Figure 12. Ingrowth to steady-state activities for  $^{224}\text{Ra}$  (A) and  $^{223}\text{Ra}$  (B) for the three marshes: Wertheim 1, Wertheim 2, and Seatuck.

Pore water residence times for each of the three marshes can then be estimated by solving for  $\tau$  on eqn. 4 (Table 1):

$$\tau = \ln [(1 - (^{224, 223}\text{Ra} / P'_{224, 223})) * 1 / (-\lambda^{224, 223})] \quad [9]$$

**4.1.2. Pore water Residence Times based on  $^{224}\text{Ra}$ :** The results suggest that for Wertheim 1, the average residence times for summer was  $\sim 3$  days for both; 20 cm and 120 cm, while for the early winter samples were  $\sim 3$  days at 20 cm and  $\sim 20$  days at 120 cm (Fig. 13A). The averages of pore water residence times for summer samples at Wertheim 2 were  $\sim 2.6$  days at 20 cm and  $\sim 1.4$  days at 120 cm, while for winter samples were  $\sim 2$  days at 20 cm and  $\sim 1$  days at 120 cm (Fig. 13C) (Table 1).

The averages for pore water residence time for summer samples at the Seatuck site were  $\sim 6$  days at 20 cm and  $\sim 2.6$  days at 120 cm, while the winter samples were  $\sim 6$  days at 20 cm and  $\sim 5$  days at 120 cm (Fig. 13E) (Table 1).

The results for pore water residence times showed different spatial and temporal values between and within marshes. These differences were apparent even between Wertheim 1 and 2, which are located within the same marsh system and influenced by the same river, Carmans River, presumably the same sources of groundwater, bay water, and tidal regime. Wertheim 1 shows similar values for pore water residence times during summer at the mid-marsh and marsh interior, however deep samples had lower residence times, while the marsh edge shows shorter residence time at 20 cm than at 120 cm (Fig. 13A). Wertheim 2 shows shorter residence times at 20 cm than at the marsh edge for winter and the opposite for summer, while the mid-marsh and marsh interior had longer residence times at 20 cm depth than at 120 cm. The Seatuck site shows a decreasing pattern for both; summer and winter on pore water residence times from the marsh edge toward the marsh interior, however the pattern is more accentuated for summer than winter (Fig. 13E).

**4.1.3. Pore water Residence Times based on  $^{223}\text{Ra}$ :** The results for Wertheim 1 show an average pore water residence time for summer of  $\sim 2$  days at 20 cm and  $\sim 1$  day at 120 cm, while for the early winter samples were 2.6 days at 20 cm and  $\sim 2$  days at 120 cm (Fig. 13B). Wertheim 2 shows average pore water residence times for summer of  $\sim 1.4$  days at 20 cm and  $\sim 2$  day at 120 cm, while for early winter samples were  $\sim 1$  day at 20 cm and  $\sim 0.6$  days at 120 cm (Fig. 13D).

The Seatuck site, a non-restored marsh, presents average pore water residence times for the summer samples of  $\sim 3.6$  days, at 20 cm and  $\sim 3$  days at 120 cm, while the winter samples were  $\sim 5.6$  days at 20 cm and  $\sim 4$  days at 120 cm (Fig. 13F)

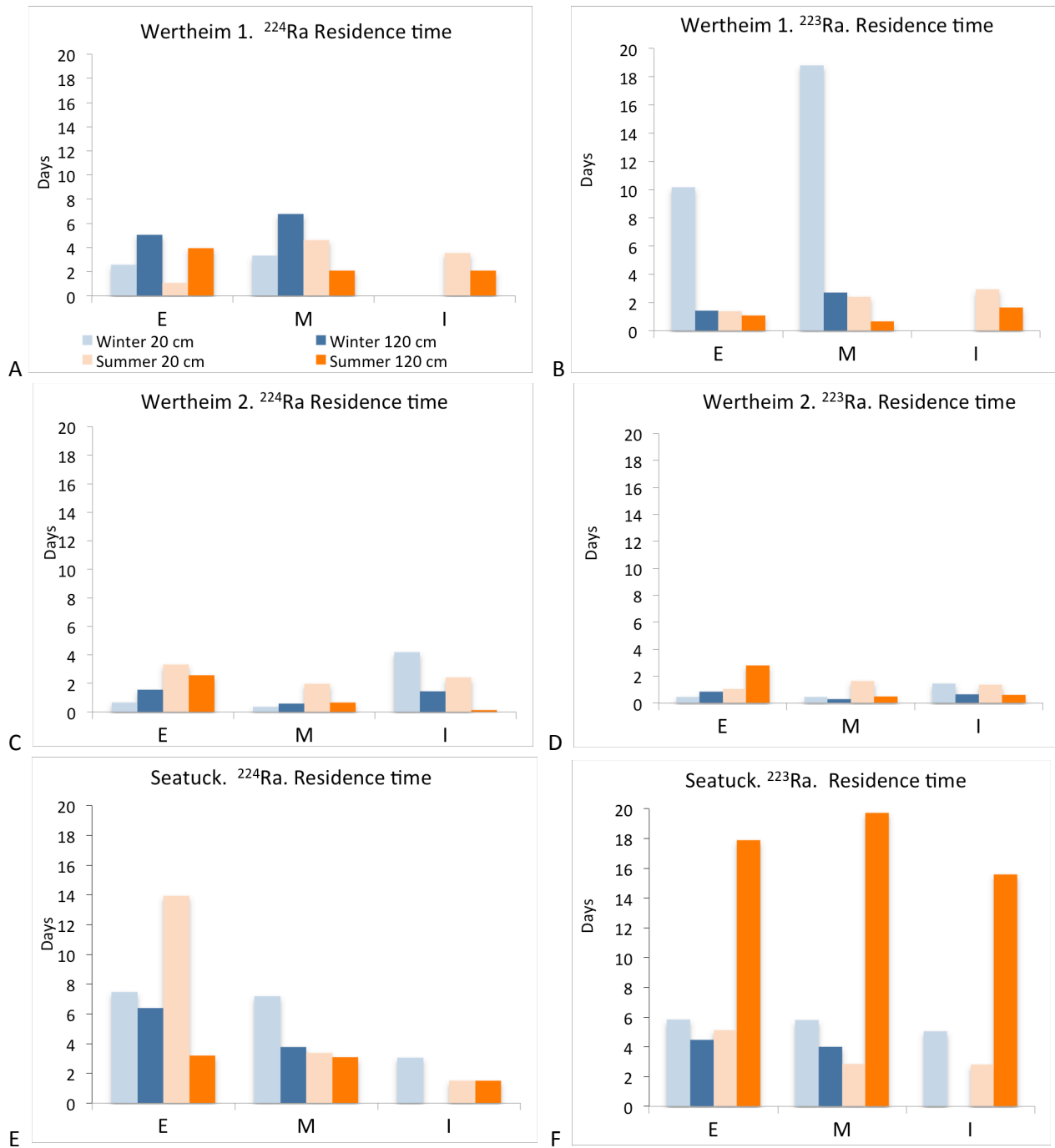


Figure 13. Pore water residence times determined based on  $^{224}\text{Ra}$  (A, C, E) and  $^{223}\text{Ra}$  (B, D, F) for summer and winter samplings. E: Marsh edge, M: Mid marsh, I: Marsh interior. ■: 20 cm Summer, ■: 120 cm Summer, ■: 20 cm Winter, ■: 120 cm Winter.

A cross plot of  $^{224}\text{Ra}$  and  $^{223}\text{Ra}$  pore water residence times for all marshes and the linear correlation is shown on figure 14. Values of pore water residence time determined by  $^{223}\text{Ra}$  were in general lower than those calculated from  $^{224}\text{Ra}$ . The differences could be due to the estimated  $^{227}\text{Th}$  activities ( $^{223}\text{Ra}$  parent) from the solid phase U. As noted above, the U activities seemed to be high, which is possibly the result of uptake of U as pore water flows through the marsh. Uranium uptake by the marsh likely would result in the  $^{235}\text{U}$  series not reaching equilibrium through  $^{231}\text{Pa}$  (half-life = 32,760 years) and its daughters (e.g.  $^{227}\text{Th}$ ). Thus the actual  $^{227}\text{Th}$  activities in the solids would be overestimated. This produces an overestimated production rate, and steady-state pore water value, and as a result shorter  $^{223}\text{Ra}$  residence times and higher than predicted  $^{224}\text{Ra}/^{223}\text{Ra}$  ratios in the pore water. For that reason, we are more confident of the use of  $^{224}\text{Ra}$  approach to determine pore water residence times for the three marshes. Despite the uncertainties, the estimated pore water residence times at the marshes studied are typically less than about 1 week.

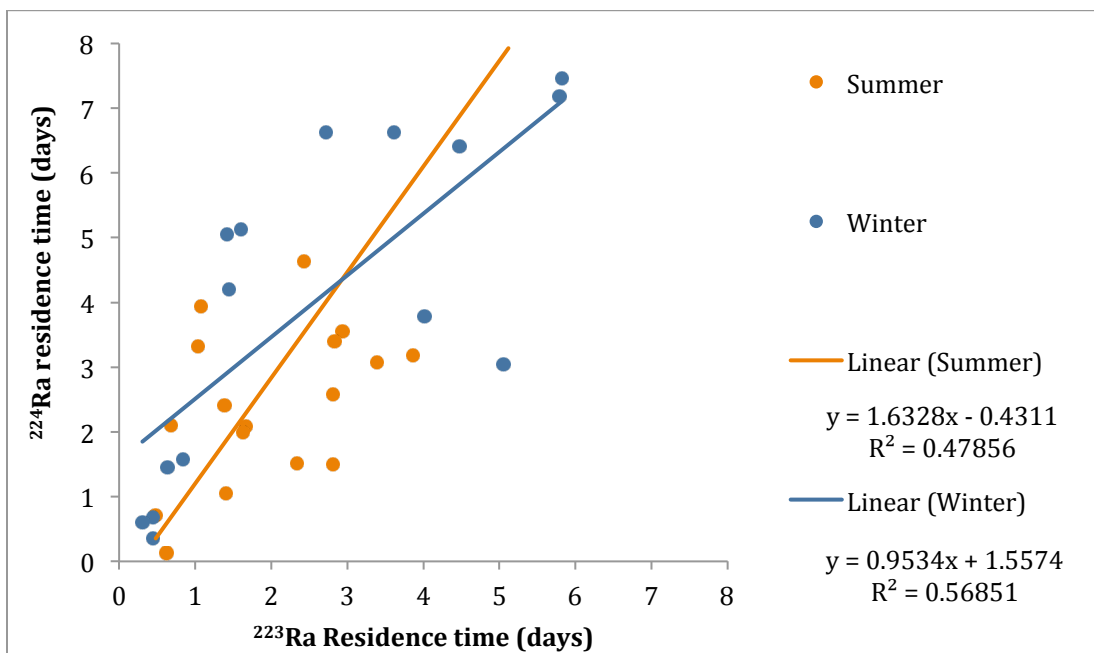


Figure 14. Linear relationship between pore water residence times determined by  $^{224}\text{Ra}$  versus  $^{223}\text{Ra}$  for summer (orange) and winter (blue). Values for  $^{224}\text{Ra}$  and  $^{223}\text{Ra}$  include the three marshes.

**4.1.4. Possible effects of salinity on pore water Ra activities:** Desorption of Ra from particles to marsh pore water can be influenced by salinity, thus variations in salinity can represent an



important factor on pore water residence times. The relationship between pore water residence times ( $^{224}\text{Ra}$  age) and salinity (Fig. 15) shows a similar distribution to the one between Ra activities and salinity shown on Fig. 6. For a given pore water residence time and value of P, Ra activities would be expected to increase with increasing pore water salinity and consequent lower K. However, the  $^{224}\text{Ra}$ -derived pore water residence times (calculated assuming a constant value of K) do not show a clear relationship with salinity, at least at the Wertheim marshes (Fig. 15). In order to better evaluate a linkage between pore water salinity and residence times, more samples would be needed, including more detailed vertical profiles and with less distance between samples so to identify a clear freshwater-saltwater interface zone.

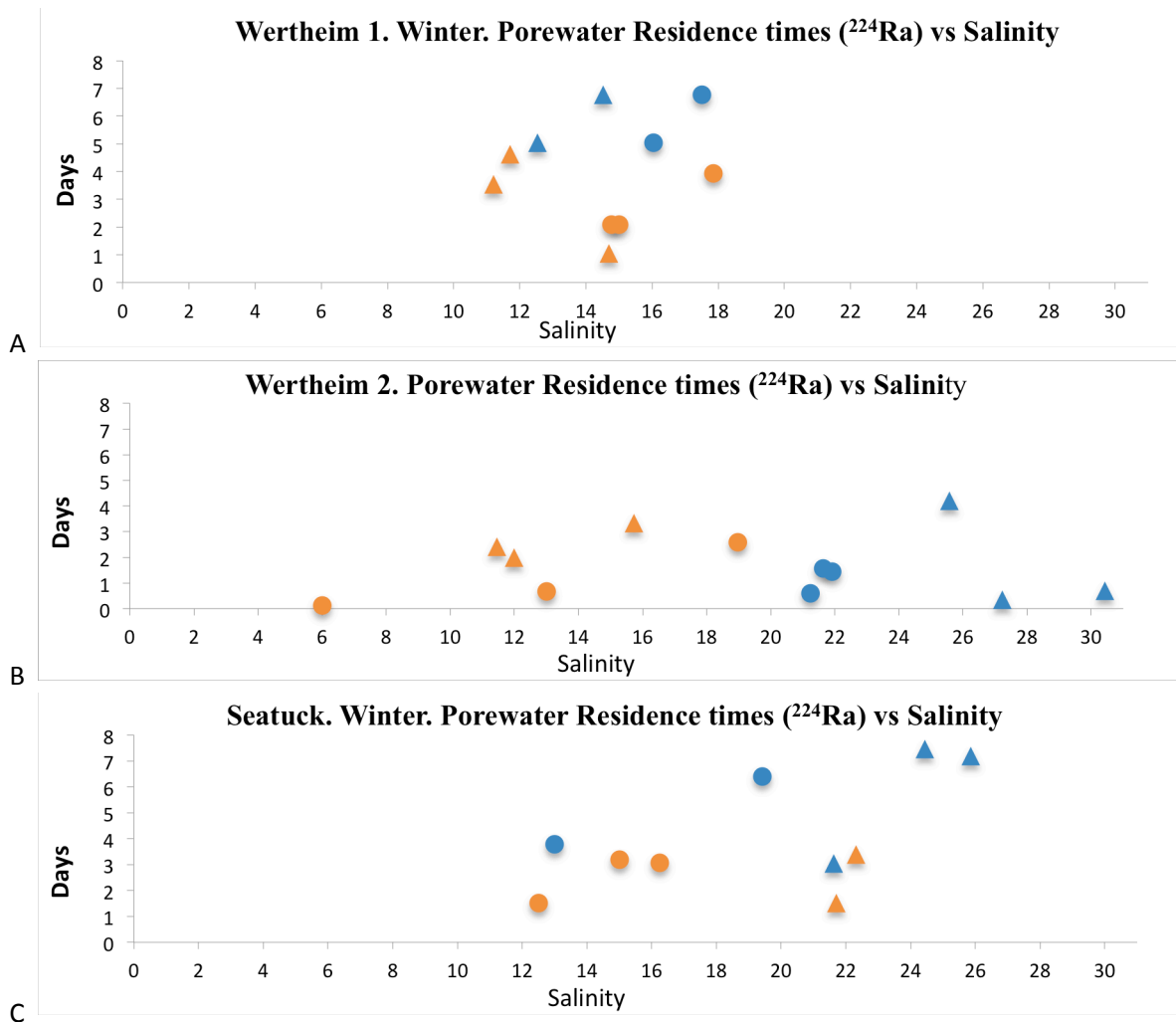


Figure 15.  $^{224}\text{Ra}$ -derived pore water residence times versus Salinity (PSU) for summer and winter for Wertheim 1 (A), Wertheim 2 (B), and Seatuck (C). Series symbols:  $\blacktriangle$ : 20 cm Summer,  $\bullet$ : 120 cm Summer,  $\blacktriangle$ : 20 cm Winter,  $\bullet$ : 120 cm Winter.

**4.2 Intra- and inter-marsh variations in pore water residence times:** Of the three marshes studied, only Wertheim 1 has been restored by integrated-marsh management methods, which are mainly realized by naturalization of tidal ditches connected to fish habitat ponds within the marsh interior, replanting of marsh vegetation, and control of invasive plant species. Wertheim 2 and Setauck have not been restored, and of the two, Seatuck had been identified as in need of restoration due its degraded conditions (personal communication: Monica Williams, Biologist, Wertheim NWR, USFWS).

The results suggest that for Wertheim 1, the average residence times fall within a range of 2 to 4 days, with the exception of pore water from the marsh edge at 20 cm depth in summer with lower residence time than the rest of the samples (1.1 days). This flow patten agrees with the simple flow conceptual model of the hypothesis, which assumes that time scales of flow are faster (and thus pore water residence times will be shorter) in sites close to tidal channels and near the marsh surface. In general the marsh drainage seems to flow at similar proportions through the marsh and variations could be more the result of seasonal sources of incoming fresh groundwater and river water. The shallow depth samples at the marsh edge for summer and winter had shorter residence times than deep samples, this could be due to a possible drainage effect given by the proximity to the tidal channel.

The Wertheim 2 marsh shows pore water residence times within a range of about 4 days, however the spatial and temporal distribution was more evident than at Wertheim 1, with shorter residence times for samples collected at 20 cm at the marsh edge and mid-marsh in winter while the opposite was detected for summer. Longer residence times were also detected for summer at Wertheim 2, which could also be the effect of seasonal variation on river water and groundwater. At Wertheim 2, longer pore water residence times were found during summer at the marsh edge toward the mid-marsh at shallow depths, suggesting less effective drainage at the edge and a preferential drainage at the mid-marsh. This observation seems to indicate that during summer the drainage of the marsh is more characterized by deep flow (120 cm) rather than shallow groundwater (20 cm). As it was noticed for Wertheim 1, for Wertheim 2 the winter samples show shorter pore water residence times for the shallow depth at the marsh edge adjacent to the tidal channel, suggesting a possible drainage effect given by the proximity to the tidal channel.

The two Wertheim sites are part of the same marsh system (Wertheim 1 and Wertheim are ~600 meters apart), both influenced by the same sources of fresh water from the Carmans River and potentially the same groundwater sources, as well as the same source of bay water and tide regime, therefore the differences in marsh drainage could be attributed to physical differences between the marshes.

The Seatuck site, a non-restored marsh, had a broader range of pore water residence time of about 13.5 days, including summer and winter samples. The pore water residence times for Seatuck show a decreasing pattern from the marsh edge toward the marsh interior, and this was more accentuated in summer than winter. In general, residence times were longer at 20 cm, and also longer in winter than summer, however the longest residence time was found at the marsh edge 20 cm depth in summer. The drainage on this marsh does not follow a clear pattern, although preferential drainage can be assumed for deep samples for summer and winter.

Wertheim 1 had an overall pore water salinity of 20.5 for the summer samples and 22 for winter samples, however salinities were higher at 120 cm throughout the study. The salinity pattern observed at Wertheim 1 could be due to the physical characteristics of the site as it was subject to Integrated Marsh Management restoration through which ditched channels within the marsh were interconnected to fish reservoirs that do not dry out through the tidal cycle. These hydrological features allow fresh water from the Carmans River to be mixed with bay water, thus inundating the surface area of the marsh and sipping through the marsh sediments. The higher salinities observed for deep samples may be correlated to the incoming bay water entering the marsh through groundwater flow.

Wertheim 2 had an overall pore water salinity of 13 for the summer samples and 24.7 for the winter samples, however pore water salinities were higher at 20 cm depth, with the exception of the marsh edge in summer for which salinity was slightly higher at 120 cm. This observation may indicate a tidal channel effect at the marsh edge during summer, as well as the lack of hydrological features present at Wertheim 1, such as tidal ditches and fish reservoirs connected to the main tidal channels. These observations may indicate a more significant influence of bay water over the surface area of the marsh than the fresh water from the Carmans River mixing with the bay water at the Wertheim sites area.

The observed lower salinities on deep samples (120 cm) can be an indication of fresh groundwater flow from the inland influencing deep flow. These observations may suggest that the Integrated Marsh Management restoration applied over Wertheim 1 could be allowing the brackish water resulting from fresh water from the Carmans River mixing with bay water, to reach the interior of the marsh through the restored hydrological features, thus influencing the drainage of the marsh by providing a vertical flow that mixes with the deeper horizontal flow.

Rochlin et al. (2012b) indicate that monitoring data prior and after implementing the IMM restoration on Wertheim, shows significant differences on groundwater salinity between the restored marshes (includes Wertheim 1 this study) and the control marshes (includes Wertheim 2 this study), thus no significant effect was noted on groundwater salinity by the IMM restoration practices. However, Rochlin et al. (2012b) consider groundwater salinity from a 2 cm to about 15 cm as measured from the water table profile. As previously indicated, this study found spatial and temporal differences between pore water salinities at 20 cm and 120 cm depth between Wertheim 1 and Wertheim 2.

The overall pore water salinities at Seatuck were 18.3 for summer and 20.9 for winter. Salinities were higher for the shallow samples (20 cm) for both; summer and winter. This observation may indicate that the surface area of this marsh could be influenced by a prolonged inundation of the marsh surface with the tidal cycle. As a visible observation of this marsh site, during the sampling events this marsh had several small ponds or shallow open water features that form as the high tides inundate the marsh. Some ponds persist through the tidal cycle, while others ponds are more ephemeral and can dry out at low tide, which can increase the salinity of the sediments as patches of high salinity areas where there is the possibility of die back marsh to develop as marsh vegetation is affected by those conditions.

The results and observations indicate that the pore water residence times observed for winter at Wertheim 1 approximates the hypothesis with marsh drainage described as pore water residence times, that seems to flow faster (shorter pore water residence times) in sites close to tidal channels and near the marsh surface (Fig. 16A). The observations for summer at Wertheim 1 show faster pore water flow at shallow depth at the marsh edge, however the opposite was observed for the mid and marsh interior (Fig. 16B).

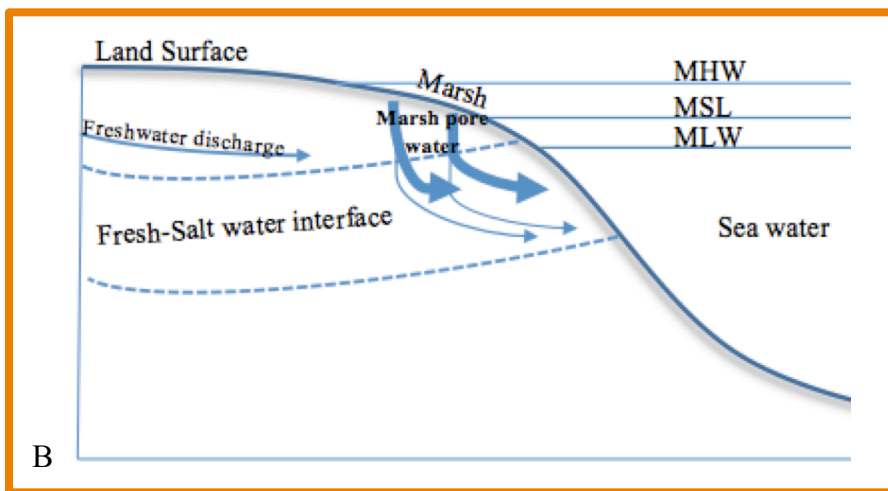
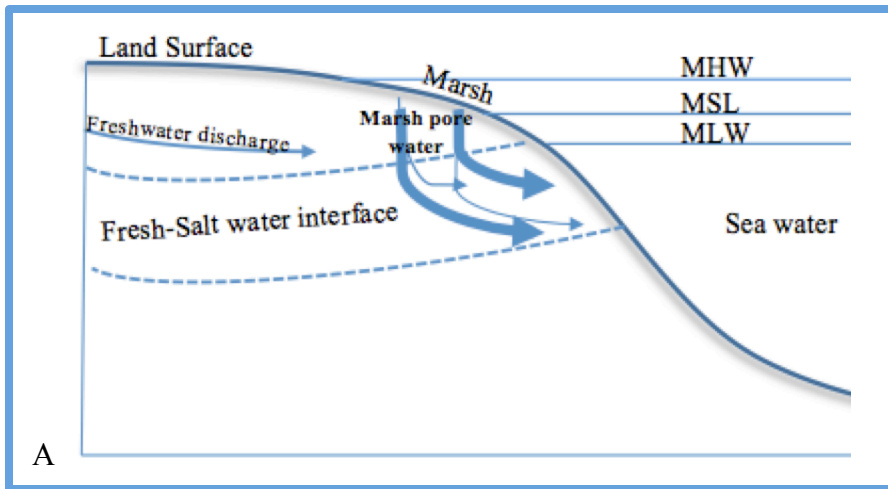


Figure 16. Pore water flow observed for Wertheim 1 based on the simple model for pore water flow. Thicker arrows indicate faster flow or shorter pore water residence times. The interface area of fresh and salt water mixing is assumed as this study sampled at just two depths. A: winter, B: summer. MHW: mean high water, MSL: mean sea level, MLW: mean low water.

The pore water residence times and drainage observed for Wertheim 2 and Seatuck do not fit the description of the hypothesis and pore water flow model. The spatial and temporal differences between and within the studied marshes indicate that the hydrological aspects that characterize the drainage and pore water residence times are indeed a variety of specifics and localize complex features. Although this study is not determining differences between marshes restored through IMM and those that are not, the results show a promising way to study those differences.

The topography of Seatuck is evidently more irregular than that of the Wertheim sites, and this characteristic is a factor on the formation of the intermittent ponds in Seatuck that are not connected to tidal channels or ditches.

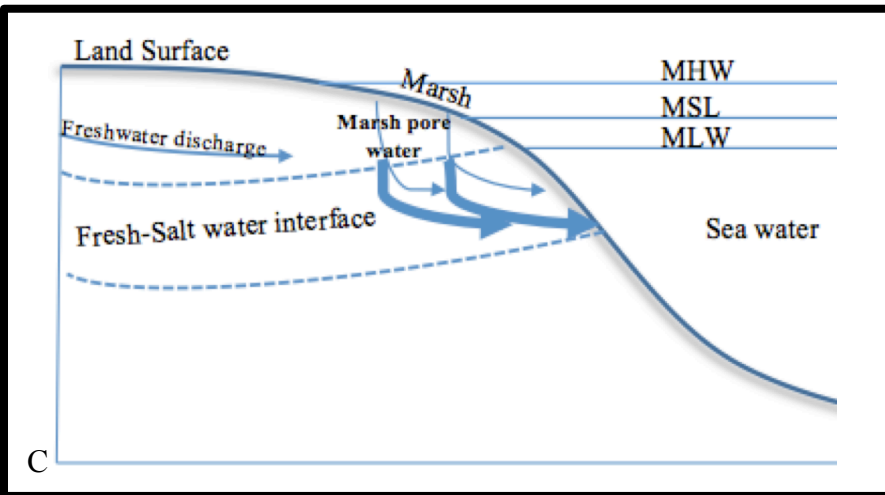
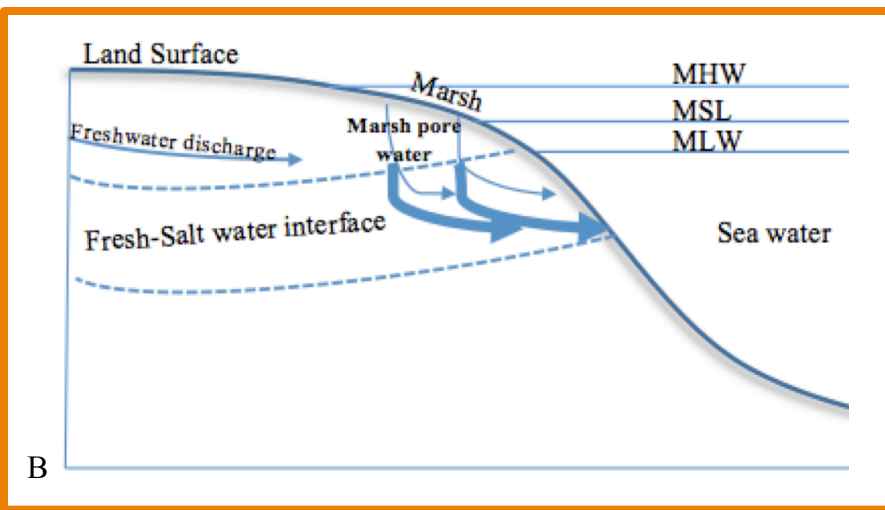
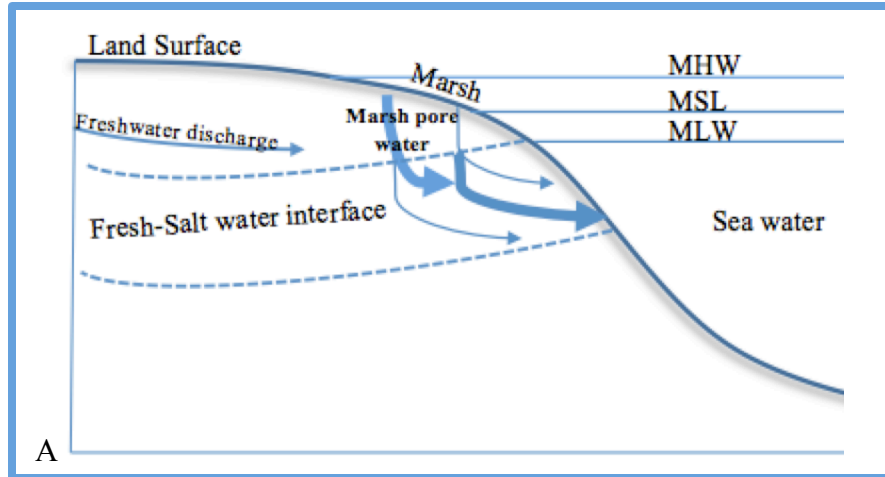


Figure 17. Pore water flow observed for Wertheim 2 and Seatuck based on the predicted model. Thicker arrows indicate faster flow or shorter pore water residence times. The interface area of fresh and salt water mixing is assumed as this study sampled at just two depths. A: Wertheim 2 winter, B: Wertheim summer, C: Seatuck summer, and winter. MHW: mean high water, MSL: mean sea level, MLW: mean low water.

The previously indicated differences in pore water residence times, drainage, and salinities between the Wertheim sites could be an effect of the restoration practices applied over Wertheim 1 but not on Wertheim 2. Integrated Marsh Management (IMM) was applied on Wertheim 1 as a demonstration restoration project in 2004 by USFWS and Suffolk County and Wertheim 2 (this study) was used as a control site for post-project monitoring activities (Rochlin et al., 2009, 2011, 2012a). Rochlin et al (2012b) state that the area corresponding to Wertheim 1 on this study was characterized by degraded conditions prior to the implementation of the restoration practices on 2004, due to restricted tidal flow, high *Phragmites australis* cover, and significant fresh groundwater input from inland.

The marshes subjected to IMM at Wertheim showed a decreased mosquito production as there was an increase of nekton (i.e. killifish) abundance in the marsh interior as a result of the hydrological features (tidal ditches, ponds) connected to the main tidal channels, and a reduction of common reed (*Phragmites australis*) with an expansion of native marsh vegetation (Rochlin et al., 2012b). Aerial imagery of the Wertheim sites before and after the implementation of the IMM practices shows the distribution of the created hydrological features on the marsh surface of Wertheim 1 in comparison to Wertheim 2 (Fig. 18).



Figure 18. Aerial view of the Wertheim areas in 2004 (pre-restoration) and 2013 (post-restoration). A: Wertheim 1 2004, B: Wertheim 1 2013, C: Wertheim 2 2004 (center), D: Wertheim 2 2013 (center).

The physical alterations that are implemented through marsh restoration practices as on IMM, are usually monitored for environmental effects over the surface area of the marsh, such as nekton, tidal regime, and vegetation cover. This study shows the need to explore the effects of IMM on the hydrogeological characteristics of marshes, such as pore water residence times and drainage.

## 5. Conclusions

This study represents one of the first to characterize drainage and pore water residence times in salt marshes using short-lived radium isotopes. This was accomplished by adapting models for advective transport of chemical species in groundwater, to the local conditions of the studied marshes. The approach and methods are based on the principle that steady state  $^{224,223}\text{Ra}$  activities in the pore water are determined by 1) recoil after their production from decay of their parent nuclides,  $^{227}\text{Th}$  and  $^{228}\text{Th}$ , in the solid phase, 2) adsorption back onto the grains after introduction into the pore water, 3) decay, and 4) any loss (export) due to flow out of the marsh peat. Furthermore, the results for short-lived Ra activities and salinities at the two sampled depths for all stations and marshes indicate a possible lateral flow through the marshes as a function of possible fresh ground water flowing through the systems.

Marsh pore water flow through marsh sediments can be caused by several factors such as tidal pressure during tidal inundation over the marsh, increased hydrostatic pressure at depth during low tide, bioturbation and marsh irregular topography, and groundwater flow from land sources directed by aquifer sediment structures, shallow confined permeable layers, and hydraulic head (Taillefert et al. 2007). These factors can create freshwater/saltwater interface areas also dependent of localized drainage dynamics for each marsh unit. In addition, the adsorption coefficient ( $K_D$ ) of Ra in brackish and salt water decreases rapidly ( $K_D \approx 10^1$ ) relative to fresh water ( $K_D \approx 10^3$ ) as the ionic strength increases (Rama and Moore, 1996; Xu et al., 2013). Therefore, radium desorption affected by higher salinity values could affect pore water residence times as traced by  $^{224,223}\text{Ra}$ .

During this study the salinity values at Wertheim 1 were lower than those for Wertheim 2. Rochlin et al. (2012b) monitored the Wertheim marshes before and after marsh restoration, and



report low salinity values for the area that corresponds to Wertheim 1 within a range of 12 to 14, in comparison to the other restored and reference sites within the Wertheim system. Rochlin et al (2012b) indicates that the low salinity in this area is caused by proximity to the brackish water from the Carmans River and fresh groundwater sources from upland sources. The area of Wertheim 1 is influenced by a more pronounced hydraulic head than Wertheim 2, as there is a gradient of elevation (high to low) from the north-east of Wertheim 1 towards the marsh (Fig. 19). Although hydraulic head was not determined on this study, the expected direction of the fresh groundwater flow is more pronounced towards Wertheim 1 assumed by the elevation gradient shown on figure 19. Therefore the low salinities and Ra values through the marsh can be supported by the expected lateral fresh groundwater flow on Wertheim 1.

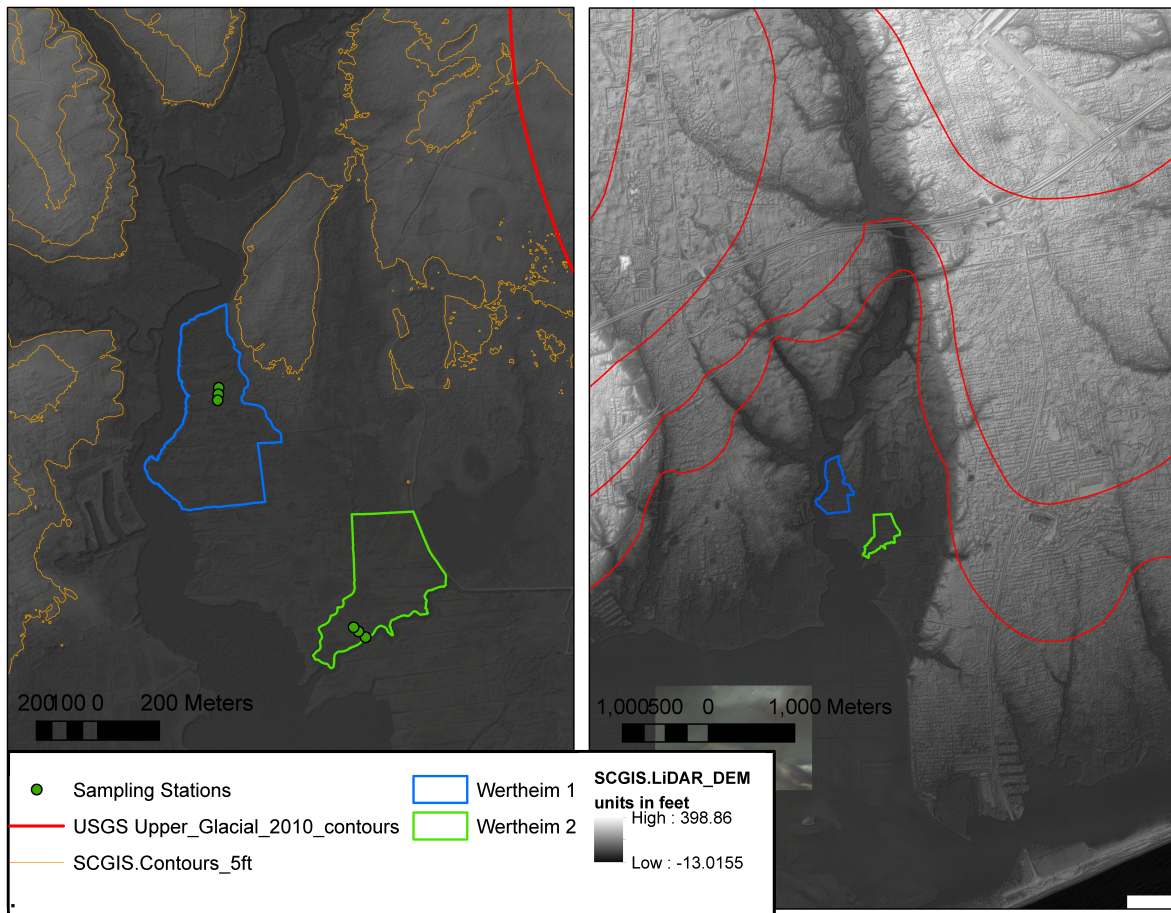


Figure 19. Elevation contour (5 ft) and depth to Upper Glacial Aquifer (data from USGS) over a Digital Elevation Model (DEM) (data from Suffolk County) for Wertheim 1 and 2. This figure shows a possible fresh groundwater influence over Wertheim 1 (blue) from the area north-east from the site, as compared with Wertheim 2.

The characterizations of marsh drainage and pore water residence times presented here for the three marshes shows variability within and between marshes. This is true even between Wertheim 1 and Wertheim 2 located about 600 meters apart, indicating that marsh drainage depends on many localized factors for each independent marsh, such as sources and flow of fresh water as groundwater and river water, tidal dynamics, marsh topography, tidal ditch network over the marsh area, and sediment structure.

The approach developed by this study has potential for the better understanding of hydrodynamics in marshes based on their geochemistry and local conditions, as well as to enhance our understanding on the effects of marsh restoration that involved the modification of hydrological feature. However, this approach as a method to characterize drainage and pore water residence times would need to be further explore and applied to other systems.

The results and observations of this study suggest different drainage and pore water hydrological dynamics for the restored marsh site relative to the non-restored marsh characterized by shorter pore water residence times at shallow depth (20 cm) of the marsh edge with the tidal channel and longer residence times at deeper flow (120 cm), while the opposite was found for the non-restored marshes. The results also showed that the mid marsh and interior marsh pore water for all marshes had longer residence times for shallow samples than for deeper samples, which we assume may be an indication of different sources and/or flow of terrestrial groundwater for each marsh.

The method used to age marsh pore water at different depths could have the potential to study and compare marsh systems that require restoration or to examine how a marsh responds to modifications made through restoration activities. Most tidal marsh post-restoration activities look at the responses of the surface area of the marsh to restoration methods such as Integrated Marsh Management. However, geochemical processes at shallow marsh peat depths, including the rhizosphere of low-to-intertidal marsh vegetation, and the role of the subterranean estuary in marshes are not fully understood or taken into account. Therefore there is a significant need for geochemical methods that can be integrated into before and after restoration projects and improve our understanding of marsh hydrology.

This study has applied short-lived Ra isotopes,  $^{224,223}\text{Ra}$ , as tracers for pore water residence time

with the assumption that Ra activities are at steady state as determined by their production by radioactive decay of their parents  $^{227,228}\text{Th}$ , and any loss is due to decay, adsorption, and advective flow. The high complexity of intertidal marsh sediments geochemistry can be affected by several factors such as sediment transport, tidal pumping, wave action, bioturbation, microbial processes, and chemical processes (oxidation-reduction, adsorption) (Taillefert et al., 2007). The significance of each of these factors independently and/or combined, as well as the hydrodynamics of groundwater flow and drainage in marshes, are determined by very localized conditions.

The need for appropriate marsh restoration practices has been increasing as marshes in Long Island have been losing acreage, with the conversion from high marsh to intertidal marsh, a net loss of high marsh areas and the formation of pannes and ponds (pools) as wet depressions within marshes and isolated from tidal channels. Pools are usually deeper than pannes and tend to retain water through the summer, while pannes do not. Under high evaporation rates some pannes and ponds can have high salinity levels, which can affect the marsh vegetation and overall biology.

The marsh loss rate between 1974 and 2008 in Long Island has been estimated to be from 10.5 to 23.8, and has been mostly attributed to a substantial subsidence/drowning of tidal marshes throughout Long Island's three major estuary systems, Long Island Sound, Peconic, and South Shore (unpublished data, New England Interstate Water Pollution Control Commission, Long Island Wetlands Trends Analysis). Marsh drowning/waterlogging leads to poor accretion processes such as biological and mineral deposition of sediments and accumulation of plant biomass and marsh subsidence in addition to physiological stresses such as increased flooding, sulfide accumulation, and nutrient enrichment (Wigand et al. 2014). The Integrated Marsh Management project conducted on the Wertheim NWR was monitored from 2004 to 2014 (Rochlin et al. 2009, 20012a, 2012b) and will be used as a basis for future restoration projects in the Long Island (personal communication, Monica Williams, USFWS).

This study observed that drainage at Wertheim 1 was greater (i.e. lower pore water residence times of ~3 d) at shallow depth (20 cm) in both summer and winter. The drainage at 120 cm was seasonally variable for Wertheim 1. In comparison, Wertheim 2 had preferential drainage for

deep flow (120 cm) with ~1.4 days (and 12 salinity) and ~1 days (and 22 salinity) for summer and winter respectively. Although it is not possible to establish a cause-and-effect relationship between the modified hydrological features on Wertheim 1 and the preferential drainage flow on shallow depths, it is possible that the vertical flow given by tidal inundation through the marsh sediment could be related to the lateral flow at shallow depths.

In general, monitoring data before and after marsh restoration have included information on the area of surface vegetated marsh and tidal channels. The geochemical approach developed in this study can augment such data and improve our understanding of marsh drainage dynamics before and after marsh restoration.

Table 1. Results for Ra isotopes (dpm/100 L) and water quality parameters in the pore water for all the marshes: salinity (‰), temperature (°C), and dissolved oxygen (mg/L)

		SUMMER SAMPLING					WINTER SAMPLING					Summer			Winter				
		Depth	<sup>224</sup> Ra (dpm/100L)	<sup>224</sup> Ra Residence Time	<sup>223</sup> Ra (dpm/100L)	<sup>223</sup> Ra Residence Time	<sup>224</sup> Ra / <sup>223</sup> Ra	<sup>224</sup> Ra (dpm/100L)	<sup>224</sup> Ra Residence Time (d)	<sup>223</sup> Ra (dpm/100L)	<sup>223</sup> Ra Residence Time (d)	<sup>224</sup> Ra / <sup>223</sup> Ra	Salinity (PSU)	T (°C)	DO (mg/L)	Salinity (PSU)	T (°C)	DO (mg/L)	
Wertheim -1	Tidal Ditch		19.2		2.8		6.9		34.1		5.2		6.6	8.1	26.5	4.5	8.74	8.49	5.9
	Marsh Edge	20 cm	94.8	1.1	10.1	1.4	9.4	326.7	5.1	11.5	1.6	28.4	14.7	27.2	1.47	12.54	9.91	4.9	
		120 cm	276.1	3.9	7.8	1.1	35.4	323.1	5.0	10.2	1.4	31.8	17.85	26.75	2.45	16.04	8.95	5.2	
	Mid- marsh	20 cm	306.6	4.6	17	2.4	18.1	375.5	6.6	24.4	3.6	15.4	11.7	25.68	5.61	14.52	8.5	5	
		120 cm	172.3	2.1	5	0.7	34.5	531.4	35.9	18.8	2.7	28.2	15	21.15	1.28	17.5	8.85	4.8	
	Marsh Interior	20 cm	257.2	3.6	20.2	2.9	12.7						11.2	23.25					
120 cm		171	2.1	11.9	1.7	14.4						14.78	21.02						
Wertheim -2	Tidal Ditch		4.5		2.7		1.6		15.3		0.6		25.5	8.4	27	4.5	15.2	17.3	5.6
	Marsh Edge	20 cm	295.4	3.3	5.3	1.0	56	76.8	0.7	2.3	0.4	32.8	15.73	27.01	1.47	30.42	17.4	2.09	
		120 cm	244	2.6	13.6	2.8	17.9	163	1.6	4.3	0.8	37.6	18.97	26.95	2.45	21.63	17.3	0.77	
	Mid- marsh	20 cm	198.8	2.0	8.2	1.6	24.2	40.9	0.4	2.3	0.4	17.8	12	24.85	5.61	27.22	16.75	0.9	
		120 cm						68.1	0.6	1.6	0.3	41.6				21.25	17.35	0.75	
	Marsh Interior	20 cm	232	2.4	7	1.4	24.2	347	4.2	7.3	1.4	47.4	11.45	22.5	1.54	25.58	16.81	1.25	
120 cm		15.4	0.1	3.2	0.6	4.9	151.8	1.5	3.3	0.6	45.3	6	19.21	4.7	21.92	17.45	0.92		
Seatuck	Tidal Ditch		39.1		3.2		12.2		19.1		1.1		17.4	20.5	26.5	5.5	21.36	3	9.15
	Marsh Edge	20 cm	530	13.9	18.4	5.1	28.7	431.5	7.5	20.5	5.8	21	22.15	25.11	1.7	24.45	2.85	6	
		100 cm	258.1	3.2	14.4	3.9	17.9	400.8	6.4	16.4	4.5	24.5	15	25.2	1.5	19.41	4.5	4.1	
	Mid- marsh	20 cm	270.2	3.4	10.9	2.8	24.7	424.2	7.2	20.4	5.8	20.7	22.31	26.6	1.74	25.85	3.2	6.05	
		120 cm	251.5	3.1	12.8	3.4	19.7	291.7	3.8	14.9	4.0	19.6	16.25	26.66	1.28	13.01	5	5.3	
	Marsh Interior	20 cm	141.6	1.5	10.8	2.8	13.1	249.9	3.0	18.2	5.1	13.7	21.7	26.9	1.15	21.63	3.47	5.39	
120 cm		141.8	1.5	9.1	2.3	15.6						12.5	26.88	1.17					

Table 2: Solid phase radiochemical data and <sup>224,223</sup>Ra production rates.

Marsh	Location	Depth (cm)	<sup>226</sup> Ra (dpm/g)		<sup>228</sup> Ra (dpm/g)		<sup>234</sup> Th ( <sup>238</sup> U) (dpm/g)		<sup>228</sup> Th (dpm/g)		<sup>235</sup> U ( <sup>227</sup> Th) (dpm/g)		<sup>228</sup> Th/ <sup>227</sup> Th (dpm/dpm)		P <sup>224</sup> Ra (dpm/100L)	P <sup>223</sup> Ra (dpm/100L)
Wertheim-1	Marsh Edge	20	1.17 ± 0.051	0.87 ± 0.08	6.19 ± 0.25	1.26 ± 0.08	0.28 ± 0.01	4.41 ± 0.32	628	142						
		120	0.86 ± 0.051	3.08 ± 0.13	6.27 ± 0.25	1.15 ± 0.07	0.29 ± 0.01	3.97 ± 0.29	573	144						
	Mid-marsh	20	0.58 ± 0.032	0.41 ± 0.05	4.46 ± 0.14	0.87 ± 0.06	0.21 ± 0.01	4.26 ± 0.31	437	103						
		120	0.51 ± 0.035	0.68 ± 0.06	4.71 ± 0.18	0.93 ± 0.06	0.22 ± 0.01	4.31 ± 0.34	467	108						
									526*	124*						
Wertheim-2	Marsh Edge	20	1.02 ± 0.054	1.01 ± 0.08	3.32 ± 0.20	1.69 ± 0.08	0.15 ± 0.01	11.08 ± 0.87	847	76						
		120	1.40 ± 0.036	0.40 ± 0.04	3.80 ± 0.13	1.54 ± 0.05	0.17 ± 0.01	8.82 ± 0.43	771	87						
	Mid-marsh	20	0.58 ± 0.039	0.53 ± 0.06	4.10 ± 0.19	0.90 ± 0.07	0.19 ± 0.01	4.79 ± 0.45	452	94						
		120	0.62 ± 0.045	0.93 ± 0.06	4.55 ± 0.20	0.92 ± 0.06	0.21 ± 0.01	4.41 ± 0.36	462	105						
									633*	87*						
Seatuck	Marsh Edge	20	0.83 ± 0.038	0.48 ± 0.05	5.37 ± 0.16	0.97 ± 0.06	0.25 ± 0.01	3.93 ± 0.26	648	165						
		120	0.79 ± 0.021	0.58 ± 0.03	1.71 ± 0.10	0.77 ± 0.03	0.08 ± 0.00	9.73 ± 0.71	511	52						
	Mid-marsh	20	0.54 ± 0.028	0.57 ± 0.04	4.84 ± 0.14	0.78 ± 0.04	0.22 ± 0.01	3.51 ± 0.20	522	149						
		120	0.89 ± 0.031	0.63 ± 0.05	1.22 ± 0.15	0.90 ± 0.05	0.06 ± 0.01	16.05 ± 2.13	601	37						
									571**	69**						

\* Mean values; calculated using K = 4, (Eqn. 8)

\*\* Mean values; calculated using K = 3, (Eqn. 8)

Table 3. Ingrowth to steady-state activities based on calculated production rates (P) and solving for  $A_{Ra}$  applying eqn. 7:  $A_{Ra} = P'(1 - e^{-\lambda\tau})$

Time (d)	Wertheim 1			Wertheim 2			Seatuck		
	<sup>224</sup> Ra	<sup>223</sup> Ra	<sup>224</sup> Ra / <sup>223</sup> Ra	<sup>224</sup> Ra	<sup>223</sup> Ra	<sup>224</sup> Ra / <sup>223</sup> Ra	<sup>224</sup> Ra	<sup>223</sup> Ra	<sup>224</sup> Ra / <sup>223</sup> Ra
0	0	0	0	0	0	0	0	0	0
0.1	10	1	13.2	12	1	22.6	11	0	25.7
0.2	20	1	13.1	24	1	22.4	21	1	25.5
0.5	48	4	12.8	57	3	22.0	52	2	25.0
1	91	7	12.4	109	5	21.3	98	4	24.3
3	228	21	11.1	274	14	19.0	247	11	21.6
5	322	32	9.9	387	23	17.0	349	18	19.4
7	386	43	9.0	465	30	15.5	419	24	17.6
10	447	56	7.9	538	40	13.6	485	31	15.5
15	495	74	6.7	596	52	11.5	538	41	13.0
20	514	87	5.9	619	61	10.1	558	48	11.5
25	521	97	5.4	627	68	9.2	566	54	10.5
30	524	104	5.0	631	73	8.7	569	58	9.8
35	525	109	4.8	632	77	8.3	570	61	9.4
40	526	113	4.7	633	79	8.0	571	63	9.1
100	526	124	4.3	633	87	7.3	571	69	8.3
125	526	124	4.2	633	87	7.3	571	69	8.3
140	526	124	4	633	87	7	571	69	8
150	526	124	4	633	87	7	571	69	8

## References

Bokuniewicz, H. J. and, Zeitlin, M. J. (1980), Characteristics of groundwater seepage into Great South Bay. Marine Science Research Center, Special Report 35, SUNY, Stony Brook, NY, 30 p.

Beck, A. J., Rapaglia, J. P., Cochran, J. K. and, Bokuniewicz, H. J. (2007), Radium mass-balance in Jamaica Bay, NY: Evidence for a substantial flux of submarine groundwater. *Marine Chemistry* 106: 419–441.

Burnet, W.C., Bokuniewicz, H. J., Huettel, M., Moore, W. S. and, Taniguchi. (2003), Groundwater and pore water inputs to the coastal zone. *Biogeochemistry* 66: 3–33.

Charette, Matthew A., Buesseler Ken O., Andrews, J. E. (2001). Utility of radium isotopes for evaluating the input and transport of groundwater-derived nitrogen to a Cape Cod estuary. *Limnology and Oceanography*. 46(2), 465-470.

Charette, Matthew A., Buesseler Ken O., Splivallo Richard, Herbold Craig, Bollinger, Marsha S., and Moore, Willard S. (2003). Salt marsh submarine groundwater discharge as traced by radium isotopes. *Marine Chemistry* 84 113– 121.

Charette, Matthew A. and Buesseler Ken O. (2004). Submarine groundwater discharge of nutrients and copper to an urban subestuary of Chesapeake Bay (Elizabeth River). *Limnology and Oceanography*. 49(2), 376–385.

Charette, Matthew A., Sholkovitz, Edward R., Hansel, Colleen M. (2005). Trace element cycling in a subterranean estuary: Part 1. Geochemistry of the permeable sediments. *Geochimica et Cosmochimica Acta*, 69(8), 2095–2109.

Charette, Matthew A. (2007). Hydrologic forcing of submarine groundwater discharge: Insight from a seasonal study of radium isotopes in a groundwater-dominated salt marsh estuary. *Limnology and Oceanography*. 52(1), 230–239.

Charette M.A., Moore W.S. and, Burnett, W.C. (2008). Chapter 5: Uranium- and Thorium-Series Nuclides as Tracers of Submarine Groundwater Discharge. *Radioactivity in the Environment*, Volume 13. Elsevier Ltd

Church, T.M., Sarin, M.M., Fleisher, M.Q. and, Ferdelman, T.G. (1996). Salt marshes: An important coastal sink for dissolved uranium. *Geochimica et Cosmochimica Acta*, Volume 60. No. 20, pp. 3879-3887

Cochran J.K. (1979). The geochemistry of  $^{226}\text{Ra}$  and  $^{228}\text{Ra}$  in marine deposits, PhD Dissertation, Yale University, New Haven CT.

Cochran, J.K. and Krishnaswami, S. (1980). Radium, thorium, uranium and  $^{210}\text{Pb}$  in deep sea sediments and sediment pore water from the north equatorial Pacific. *American Journal of Science*, 280 (9): 849-889



Garcia-Solsona E., J. Garcia-Orellana, J., Masqué, P., and Dulaiova, H. (2008), Uncertainties associated with  $^{223}\text{Ra}$  and  $^{224}\text{Ra}$  measurements in water via a Delayed Coincidence Counter (RaDeCC). *Marine Chemistry* 109: 198–219.

Griffin, H. C. (2011). *Handbook of Nuclear Chemistry*, Second edition. Springer Reference. Chapter 13: Natural Decay Chains.

Kelly, Maggi., Tuxen, Karin A., Stralberg, Diana. (2011). Mapping changes to vegetation pattern in a restoring wetland: Finding pattern metrics that are consistent across spatial scale and time. *Ecological Indicators* 11 263–273.

Koch, F. and Gobler, C. J. (2009). The Effects of Tidal Export from Salt Marsh Ditches on Estuarine Water Quality and Plankton Communities. *Estuaries and Coasts* 32:261–275.

Kolker, A. S., et al. (2009), High resolution records of coastal systems responses to short-term sea-level variability. *Estuarine Coastal Shelf Science*. 84:4, 493–508.

Konisky RA, Burdick DM, Dionne M, Neckles HA (2006). A regional assessment of salt marsh restoration and monitoring in the Gulf of Maine. *Restoration Ecology*. 14:516–525

Krest, J. M., W. S. Moore, L. R. Gardner, and J. T. Morris (2000). Marsh nutrient export supplied by groundwater discharge: Evidence from radium measurements. *Global Biogeochem. Cyc.* 14: 167–176.

Krest, J. M. and Harvey, J. W. (2003). Using natural distributions of short-lived radium isotopes to quantify groundwater discharge and recharge. *Limnology and Oceanography*. 48(1), 290–298

Moore, W. S., and Arnold, R., (1996), Measurement of  $^{223}\text{Ra}$  and  $^{224}\text{Ra}$  in coastal waters using a delayed coincidence counter, *Journal of Geophysical Research* 101: 1321- 1329

Moore, W.S. (2000a), Ages of continental shelf waters determined from  $^{223}\text{Ra}$  and  $^{224}\text{Ra}$ . *Journal of Geophysical Research: Oceans* 105: 22117–22122.

Moore, W.S. (2000b), Determining coastal mixing rates using radium isotopes. *Continental Shelf Research*. 20: 1993–2007.

Moore, W. S., and Oliveira, J. (2008), Determination of residence time and mixing processes of the Ubatuba, Brazil, inner shelf waters using natural Ra isotopes. *Estuarine, Coastal and Shelf Science* 76: 512-521.

Moore, W. S. and Cai, P. (2013), Calibration of RaDeCC systems for  $^{223}\text{Ra}$  measurements. *Marine Chemistry* 156: 130–137 <http://dx.doi.org/10.1016/j.marchem.2013.03.002>

- Porcelli, D. (2008). Chapter 4 Investigating Groundwater Processes Using U- and Th-Series Nuclides. *Radioactivity in the Environment*, Volume 13, 2008, Pages 105-153
- Rama and Moore W. S. (1996). Using the radium quartet for evaluating groundwater input and water exchange in salt marshes. *Geochimica et Cosmochimica Acta*. 60 (23): 4645-4652.
- Rochlin, I., Dempsey M. E., Iwanejko T., Ninivaggi D. V. (2009). Geostatistical evaluation of integrated marsh management impact on mosquito vectors using before-after-control-impact (BACI) design. *International Journal of Health Geographics*. 8: 35.
- Rochlin, I., Dempsey M. E., Iwanejko T., Ninivaggi D. V. (2011). Aquatic insects of New York salt marsh associated with mosquito larval habitat and their potential utility as bioindicators. *Journal of Insect Science* 11:172 available online: [insectscience.org/11.172](http://insectscience.org/11.172)
- Rochlin, I., James-Pirri M-J., Adamowicz S. C., Wolfe R. J., Capotosto P., Dempsey M. E., Iwanejko T., Ninivaggi D. V. (2012a). Integrated Marsh Management (IMM): a new perspective on mosquito control and best management practices for salt marsh restoration. *Wetlands Ecol Manage* 20:219–232
- Rochlin, I., James-Pirri M-J., Adamowicz S. C., Dempsey M. E., Iwanejko T., Ninivaggi D. V. (2012b). The Effects of Integrated Marsh Management (IMM) on Salt Marsh Vegetation, Nekton, and Birds. *Estuaries and Coasts*. 35:727–742
- Roman C.T, Raposa KB, Adamowicz SC, James-Pirri MJ, Catena JG (2002) Quantifying vegetation and nekton response to tidal restoration of a New England salt marsh. *Restor Ecol* 10:450–460
- Simas, T., Nunes, J.P., Ferreira, J.G. (2001). Effects of global climate change on coastal salt marshes. *Ecological Modelling* 139 1–15.
- Taillefert, M., Neuhuber, S., Bristow, G. (2007). The effect of tidal forcing on biogeochemical processes in intertidal salt marsh sediments. *Geochemical Transactions*. 8(6).
- Wigand C, CT Roman, E Davey, M Stolt, R Johnson, A Hanson, EB Watson, SB Morgan, DR Dahoon, JC Lynch, and P Rafferty. 2014. Below the disappearing marshes of an urban estuary: historic nitrogen trends and soil structure. *Ecological Applications*. 24(4): 633-649
- Xu, B., Burnett, W., Dimova, N., Diao, S., Mi, T., Jiang, X., Yu, Z. (2013). Hydrodynamics in the Yellow River Estuary via radium isotopes: Ecological perspectives. *Continental Shelf Research*. 66: 19-28.
- Yang, S. (2008), Quantification of the tidal exchange of radium as an indicator of submarine groundwater inputs to Great South Bay. MS Thesis. School of Marine and Atmospheric Sciences, Stony Brook University. Stony Brook, NY.